True eddy accumulation - Part 1: Solutions to the problem of non-vanishing mean vertical wind velocity

Anas Emad[1] and Lukas Siebicke[1]

[1]Bioclimatology, University of Göttingen, Büsgenweg 2, 37077 Göttingen, Germany

Correspondence: Anas Emad (anas.emad@uni-goettingen.de)

Abstract. The true eddy accumulation method (TEA) provides direct measurements of ecosystem-level fluxes for a wide range of atmospheric constituents. TEA utilizes conditional sampling to overcome the requirement for a fast sensor response ~~usually~~ demanded by the state-of-the-art eddy covariance method (EC).

~~However, the assumptions and conditions required for the TEA method are often not met. Here we explore the limitations~~
~~caused by the assumption of~~ The TEA method is formulated under the assumption of ideal conditions with a zero mean vertical wind velocity during the averaging interval~~and by the fixed accumulation interval.~~. However, this idealization is rarely met under field conditions. Additionally, unlike in EC, this assumption can not be imposed in post processing due to the real-time nature of sampling and the absence of high-frequency measurements of the scalar. Consequently, fluxes measured with the TEA method are biased with an advective term that scales with the scalar mean concentration.

~~We extend the theory of TEA method to non-zero vertical wind velocity by employing information about the scalar transport.~~
~~We further derive a new method with adaptive time varying accumulation intervals~~ Here, we explore the magnitude of this biased advective term and potential ways to minimize or remove it. We propose a new formulation to calculate TEA fluxes that minimizes the bias term. The new ~~method, termed short-time eddy accumulation (STEA), was successfully implemented~~ ~~and deployed to measure fluxes over an agricultural field in Braunschweig, Germany. The measured fluxes matched very well~~ ~~against a conventional EC system (slope of 1.05, R^2 of 0.87). We provide a detailed description of the setup and operation of~~ ~~the STEA system in the flow-through mode, devise an empirical correction for the effect of buffer volumes, and describe the~~ ~~important considerations for the successful operation of the STEA method~~formulation shows that the magnitude of the error is constrained to $\bar{w}/\overline{|w|}$ when the stationarity criterion is fulfilled. Here, w is the vertical wind velocity, and the overbar denotes time averaging. The error is shown to be dependent on the asymmetry of atmospheric transport, represented by the coefficient α_c. Two methods of estimating the coefficient α_c are proposed, a probabilistic treatment of turbulent transport, and a method utilizing the assumption of scalar similarity. We show how other formulas for calculating the TEA flux are linked to the new formulation and explore the different corrections in a numerical simulation.

The new ~~theory developments reduce the bias and uncertainty in the measured fluxes and create new ways to design eddy~~ ~~accumulation systems with finer control over sampling and accumulation. The results encourage the application of TEA and~~ ~~STEA for~~ formulation avoids the direct dependence of the bias term on the scalar background concentration. This result increases the confidence in applying the TEA method to measuring fluxes of ~~more challenging atmospheric constituentssuch~~

~~as reactive species as well as other constituents where no fast gas analyzers are available.~~ atmospheric constituents. In particular, to scalars with a large background concentration and a small flux, analogous to a low deposition velocity of aerosols.

1 Introduction

Micrometeorological methods provide non-invasive, in situ, integrated, and continuous point measurement for ecosystem fluxes on a scale ideal for ecosystem study (Baldocchi et al., 1988; Baldocchi, 2014). Among micrometeorological methods, eddy covariance (EC) has become the de-facto method for measuring ecosystem fluxes for the past 40 years. The EC method is the most direct micrometeorological method. It is also relatively easy to set up and operate. These features have led to the wide use and adoption of the EC method at hundreds of sites worldwide, including several regional and global flux measurements networks such as ICOS and FLUXNET (Hicks and Baldocchi, 2020).

The EC method depends on the fast measurement of vertical wind velocity and the scalar concentration (such as an atmospheric constituent). The requirement for fast measurement frequency (10 to 20 Hz) limits the application of the method to a handful of atmospheric constituents where fast gas analyzers are available. Alternative methods that work for slow gas analyzers include: (i) signal downsampling methods (Lenschow et al., 1994) such as disjunct eddy accumulation (Rinne et al., 2000a; Turnipseed et al., 2009) and disjunct eddy covariance (Rinne and Ammann, 2012), and (ii) indirect methods such as flux gradient methods (e.g., Rinne et al. (2000b)) which depend on the Monin-Obukhov similarity theory (Monin and Obukhov, 1959) and the relaxed eddy accumulation (REA) ~~based on the assumption of~~ which assumes flux-variance similarity (Businger and Oncley, 1990). The true eddy accumulation method (TEA) (Desjardins, 1977) is the most direct and mathematically equivalent alternative to eddy covariance ~~.~~ among accumulation methods. Unlike EC, the TEA method requires the concentration measurements to be carried out once every averaging interval (30 minutes) ~~. For a long time, the development of the TEA method was hindered by the difficulty of fast air flow rate control and the strict operational requirements (Businger and Oncley, 1990; Hicks and McMillen, 1984). A recent improvement to the TEA method used a new type of mass flow controllers, online coordinates rotation, and several online treatments of the signal to overcome important limitations of the method's applicability (Siebicke and Emad, 2019). The new system showed a good match with a reference eddy covariance system with coefficients of determination of up to 86% and a slope of 0.98.~~ Businger and Oncley (1990). The ~~non-necessity of high-frequency measurements of the scalar in TEA , although a major advantage, introduces multiple difficulties. First and foremost, exact equality between EC fluxes and TEA fluxes is only possible when the~~ TEA method is formulated under ideal conditions assuming a zero mean vertical wind velocity ~~is assumed to be zero during the flux~~ during the averaging interval. This assumption is almost never met under field conditions and ~~the residual~~ it is not possible to enforce in post-processing due to lacking high-frequency information of the scalar concentration. As a result, the non-vanishing vertical mean velocity ~~contributes to the~~ will contribute to a systematic error in the flux. Nonzero mean vertical wind velocity is a source of error for all eddy accumulation methods, including TEA (Hicks and McMillen, 1984), relaxed eddy accumulation (REA) (Pattey et al., 1993; Businger and Oncley, 1990; Bowling et al., 1998), and disjunct eddy accumulation (DEA) (Turnipseed et al., 2009). The reported bias on the flux due to nonzero $\bar{w}$ varied with different studies and accumulation

60 methods. For TEA, Hicks and McMillen (1984) recommended that $\bar{w}$ should not exceed $0.0005\,\sigma_w$ if accumulated mass is measured and $0.02\,\sigma_w$ when concentrations are measured directly. Turnipseed et al. (2009) reported that a mean vertical wind bias of $\pm 0.25\ \sigma_w$ lead to $\pm 15\%$ ~~errors~~ mean systematic bias in the flux using the disjunct eddy accumulation method. Values reported for the REA method showed that a ~~loss~~ systematic bias of approximately 5% of the flux due to a $\bar{w}$ of $0.20\ \sigma_w$ (Pattey et al., 1993), which agrees with the recommendations of Businger and Oncley (1990). ~~Additionally, the absence of~~

65 ~~high-frequency information means any decision on air sampling such as flow rate and sampling direction is final. The lack of high-frequency information also implies that sample accumulation should happen on a time scale similar to the flux averaging interval (30 to 60 minutes). These limitations impose restrictive design considerations related to the size and function of sample accumulation reservoirs. They also dictate that the sampling apparatus needs to accommodate a large dynamic range to cover the range of wind velocities during the flux averaging interval~~ The magnitude of the residual mean vertical velocity depends on

70 the meteorological and topographical features of the measurement site and is larger in complex sites (Rannik et al., 2020).

In this paper, we ~~address these limitations of the TEA method. First, we~~ revise the theory of the true eddy accumulation ~~and extend the TEA equation to non-ideal conditions. The new generalized TEA equation allows obtaining TEA fluxes equivalent to fluxes measured with EC when the vertical wind velocity is nonzero. This is achieved by incorporating knowledge about the scalar~~ method and obtain a generalized equation that isolates the error due to nonzero vertical wind velocity. The new equation

75 shows that the error in the flux is a function of the atmospheric transport represented by the transport asymmetry coefficient. ~~We show analytical and empirical ways to obtain the transport asymmetry coefficient and provide an interpretation of its value. Then, we describe the sensitivity of the flux to values of~~ , α_c. We study the value and the interpretation of this coefficient in the framework of quadrant analysis and define its boundary conditions. Next, we show analytical and empirical ways to obtain the transport asymmetry coefficient ~~, the residual vertical mean velocity, and~~ and explore the implications of these estimates on

80 the ~~different operational conditions. Next, we derived a new TEA method, the short-time eddy accumulation (STEA), which allows to carry out the sample accumulation on variable intervals shorter than the flux averaging interval. We discuss the advantages and steps required to carry out flux measurements using the STEA method, different operational requirements, and develop an empirical correction for the use of buffer volumes.~~ flux in a numerical simulation. Finally, we show ~~a prototype and experimental measurements for fluxes using the newly developed STEA method in flow-through mode and compare the~~

85 ~~measured fluxes to reference EC measurements~~ how different formulations for calculating the TEA flux are special cases of the new equation.

2 Theory

2.1 Eddy covariance

The net ecosystem exchange (NEE) of a scalar c (such as an atmospheric constituent), $\overline{N_c}$ is the total vertical flux $\overline{wc}$ across

90 the measurement plane at a height h and the change of storage below that height (Gu et al., 2012).

$$\overline{N_c} = \overline{wc}\big|_h + \int_0^h \frac{\partial c}{\partial t}\,\mathrm{d}z \tag{1}$$

Where w is the vertical wind velocity ($\mathrm{m\,s^{-1}}$), c is the molar density ($\mathrm{mol\,m^{-3}}$) of the scalar of interest (such as CO_2). The previous equation can be reached either from a holistic mass balance approach or by averaging the continuity equation for the scalar, c and integrating from the surface to measurement height, h. In both cases, horizontal advection is ignored as a virtue of the assumption of horizontal homogeneity and molecular diffusion is ignored due to its small magnitude (Gu et al., 2012). For a full discussion on the equations of surface flux, see, for example (Finnigan et al., 2003; Foken et al., 2012a).

The storage term measurements and value are beyond the scope of this study, therefore we ignore it. Consequently, the total vertical flux is represented by the first term on the right hand side of Eq. (1) which can be further decomposed into turbulent and mean advective parts.

$$\overline{wc} = \overline{w'c'} + \overline{w}\,\overline{c} \tag{2}$$

The overlines denote ensemble averages that obey Reynolds averaging rules. Primes represent departures from the mean. The ensemble averages are estimated experimentally by ~~the~~ time averages, thus for a stationary time series drawn from an ensemble, the turbulent flux for the averaging period ~~T_{avg}~~ Δt can be written as

$$F_{T_{avg}} = \frac{1}{T_{avg}} \int_0^{T_{avg}} w'(t)c'(t)\,dt = \overline{w'c'}$$

$$F_{\Delta t} = \frac{1}{\Delta t} \int_0^{\Delta t} w'(t)c'(t)\,\mathrm{d}t = \overline{w'c'} \tag{3}$$

where $w(t)$ and $c(t)$ are realizations of the vertical wind velocity and the scalar quantity such as CO_2 concentration, respectively.

~~The first term on the right-hand side of Eq. (2) is the covariance between vertical wind velocity and the scalar concentration. It is often referred to as the turbulent flux or the first-order approximation of the eddy flux, whereas the mean vertical advective term (second term on the right-hand side of Eq. (2)) is known as "Webb correction" or Webb-Pearman-Leuning (WPL) correction (Webb et al., 1980), and exists due to fluctuations in air density (Fuehrer and Friehe, 2002). The mean vertical wind velocity induced by density fluctuations of air parcels, hereafter $\overline{w_d}$, is often nonzero and is needed to account for the mean advective term in the flux. It is, however, not possible to directly measure it. One reason is that $\overline{w_d}$ caused by air density fluctuations is rather small (less than 1). But more importantly, any offset in the vertical wind velocity will appear~~

2.2 True Eddy Accumulation

The true eddy accumulation method circumvents the need to ~~measure individual realizations of the scalar concentration~~ record the fluctuations of scalar concentration at a frequency sufficient to represent the individual flux transport eddies. Instead, it is sufficient to measure the mean product $\overline{wc}$ for updraft and downdraft once ~~at the end of~~ for each averaging interval ~~T_{avg}~~, Δt (e.g. 30 minutes).

The product of w and c is realized by physically collecting air samples with a flow rate proportional to the vertical wind velocity, w. The method is formulated assuming ideal conditions ~~,~~ where the mean vertical wind velocity during the averaging period is assumed to be zero. When $\bar{w} = 0$, the second term on the right hand side of Eq. (2) will be zero and the turbulent flux $\overline{w'c'}$ will equal the ~~mean product~~ total ecosystem flux $\overline{wc}$. By separating $\overline{wc}$ depending on the direction of the vertical wind velocity we can write

$$\overline{wc} = \frac{1}{T_{avg}} \int_0^{T_{avg}} (\delta^+ cw + \delta^- cw)\, \mathrm{d}t$$

$$\overline{wc} = \frac{1}{\Delta t} \int_0^{\Delta t} (\delta^+ cw + \delta^- cw)\, \mathrm{d}t \tag{4}$$

$$\text{where} \quad \begin{cases} w > 0 & \delta+ = 1;\ \delta- = 0 \\ w < 0 & \delta+ = 0;\ \delta- = 1 \end{cases} \tag{5}$$

Hence, by sampling air with a flow rate proportional to the magnitude of vertical wind velocity and accumulating it according to its direction in updraft and downdraft reservoirs, one can measure the quantity $\overline{wc}$ and consequently the flux without having to measure the high-frequency fluctuations of the scalar, c (Desjardins, 1977; Hicks and McMillen, 1984).

~~A simpler alternative formulation can be reached using the law of total expectation. We write the flux as the expected value of the random variable wc conditional on the direction of the vertical wind velocity $\text{sign}(w)$~~

$$\overline{wc} = \overline{\left((wc)|\text{sign}(w)\right)}$$

Sampling air proportional to the magnitude of vertical wind velocity requires a scaling parameter, A that ~~maps vertical wind velocity to the flow rate~~ensures the proportionality of the flow rate to the magnitude of vertical wind velocity. The scaling parameter is the product of the pump calibration coefficients and other coefficients used to adjust the system's dynamic range. For a short interval of time dt, a sample of the volume $V_{sample} = A|w|\,dt$ will be collected in the system.

The accumulated sample volume in each of the two reservoirs during a long enough averaging period ~~T_{avg}~~Δt (30 to 60 minutes) will be

$$V_{total} = \frac{1}{T_{avg}} \int_0^{T_{avg}} A|w|\,dt$$

$$V_{total} = \frac{1}{\Delta t} \int_0^{\Delta t} A|w|\,dt \tag{6}$$

By the end of the averaging period ~~T_{avg},~~ Δt, the flux will be equal to the difference in the scalar accumulated mass between updraft and downdraft reservoirs.

If it is desired to formulate the flux in terms of the accumulated scalar concentration ($\mathrm{mol\,m^{-3}}$) instead of the accumulated mass, the average scalar density of accumulated samples in each of the reservoirs will equal the accumulated mass of the scalar divided by the accumulated volume

$$C_{acc}^{\uparrow\downarrow} = \frac{m}{V} = \frac{A \int_0^T c\,|\delta^{\pm}w|\,dt}{A \int_0^T |\delta^{\pm}w|\,dt}$$

$$C_{acc}^{\uparrow\downarrow} = \frac{m}{V} = \frac{\overline{c\,|w^{\uparrow\downarrow}|}}{\overline{|w^{\uparrow\downarrow}|}} \tag{7}$$

Where C_{acc} is the accumulated scalar density and the arrows indicate the reservoir. The measured concentration in Eq. ~~(??)~~ 7 is the weighted mean of the scalar concentration and the magnitude of the vertical wind velocity. ~~We can simply rewrite the accumulated concentration in terms of the wind and the scalar concentration as~~

$$C_{acc}^{\uparrow\downarrow} = \frac{\overline{c\,|w^{\uparrow\downarrow}|}}{\overline{|w^{\uparrow\downarrow}|}}$$

When $\overline{w}$ is assumed to be zero, $\overline{|w^{\uparrow}|} = \overline{|w^{\downarrow}|} = \overline{|w|}/2$, and we can write the flux in terms of concentrations of accumulated samples, similar to Hicks and McMillen (1984)

$$F_{\mathrm{TEA}} = \frac{\overline{|w|}}{2}(C_{acc}^{\uparrow} - C_{acc}^{\downarrow}) \tag{8}$$

2.3 ~~Extending the TEA equation to non-ideal conditions~~

Where $\overline{|w|}$ is the mean of the magnitude of the vertical wind velocity.

~~As we discussed in Sect~~

2.3 The problem of nonzero mean vertical wind

Although the total ecosystem flux is defined to be $\overline{wc}$ in Eq. ~~(2.1), the mean advective term in Eq. (2) needs to be discarded due to the~~ 2), it is not possible to directly use the measured w and c to calculate the total flux. The reason is the difficulty of obtaining an accurate measurement of w. Any non-turbulent offset (bias) in the mean vertical velocity will lead to a flux biased with $\overline{wc}$. Several reasons contribute to a biased mean vertical wind velocity ~~.~~ including: topography in particular in complex sites, tilted coordinates, biases in instruments, flow perturbations, and meteorological reasons induced by local circulation or topographical drainage (Lee et al., 2005; Paw U et al., 2000; Heinesch et al., 2007). Therefore, the measured biased advective term needs to be discarded and the true physical term, known as "Webb term" or Webb-Pearman-Leuning (WPL) term, need to be estimated by other means (Webb et al., 1980; Fuehrer and Friehe, 2002). The original formulation of the TEA method assumes a zero mean vertical wind velocity during the flux averaging interval ~~. This~~ thus assumes the total ecosystem flux to be equal to the turbulent flux, $\overline{w'c'}$. However, this assumption is rarely valid under field conditions due to the reasons outlined earlier ~~.~~ and the measured TEA flux will be a biased total vertical flux, $\overline{wc}$. If the turbulent flux is to be measured using the TEA method, the biased term $\overline{w}\overline{c}$ needs to be removed.

Previous efforts have been focused on minimizing $\overline{w}$ to reduce the bias in the TEA flux. However, since the wind information can not be changed after sampling, any treatments for the wind velocity measurements are final when the air samples have been collected. Thus, there is no way to guarantee a zero mean vertical velocity. A common approach to ~~nullify~~ nullifying mean vertical wind velocity in EC measurements is to rotate the wind coordinates in ~~post processing~~ post-processing to force $\overline{w}$ to zero for each averaging interval, this method - commonly referred to as double rotation - is not feasible in eddy accumulation methods. The planar fit method (Wilczak et al., 2001) is better suited for the online application in the TEA method (Siebicke and Emad, 2019). The planar fit method aligns the sonic coordinates to the long-term streamline coordinates by aligning the wind vector to the plane that minimizes the sum of squares of the vertical wind velocity means for a long period of time (weeks to months). This approach, while minimizes the vertical wind velocity means of the individual averaging intervals, does not force them to be zero. Considerable spread of $\overline{w}$ values around zero can still be observed after applying the planar fit method (Sun, 2007; Rannik et al., 2020).

~~The~~

2.4 TEA equation under nonzero $\overline{w}$ conditions

The goal here is to enable measuring the turbulent flux $\overline{w'c'}$ from TEA measurements when $\bar{w} \neq 0$. The key to extending the TEA equation to ~~non-ideal case~~ conditions of nonzero $\bar{w}$ is to obtain an estimate of the scalar mean $\bar{c}$ from TEA measurements,

and consequently remove the ~~biased~~ advective term $\bar{w}\bar{c}$. We achieve this by using the weighted mean of c and $|w|$ ~~and~~ as an estimate for c after correcting for the correlation between them.

The weighted mean ~~($\bar{c}_W$)~~ of the scalar, c and ~~wind magnitude~~ the vertical wind velocity magnitude, $|w|$ can be ~~written similar to~~ obtained from TEA measurements Eq. (7)~~as~~

$$\bar{c}_W = \frac{\overline{c|w|}}{\overline{|w|}}$$

~~By decomposing~~. By decomposing $\overline{c|w|}$ into mean and fluctuating parts ~~, we can write~~

$$\bar{c}_W = \bar{c} + \frac{\overline{c'|w'|}}{\bar{w}}$$

$$\overline{c|w|} = \overline{c'|w|'} + \bar{c}\,\overline{|w|} \tag{9}$$

~~It follows that~~

$$\bar{c} = \frac{\overline{c|w|}}{\overline{|w|}} - \frac{\overline{c'|w'|}}{\overline{|w|}}$$

The value of $\bar{c}$ can be found to be

$$\bar{c} = \frac{\overline{c|w|}}{\overline{|w|}} - \frac{\overline{c'|w|'}}{\overline{|w|}} \tag{10}$$

Substituting $\bar{c}$ in Eq. (2), we can write the flux as

$$\overline{w'c'} = \overline{wc} - \frac{\bar{w}}{\overline{|w|}}\,\overline{|w|c} + \frac{\bar{w}}{\overline{|w|}}\,\overline{|w'|c'}$$

$$\overline{w'c'} = \overline{wc} - \frac{\bar{w}}{\overline{|w|}}\,\overline{|w|c} + \frac{\bar{w}}{\overline{|w|}}\,\overline{|w|'c'} \tag{11}$$

We can obtain all the terms in Eq. (11) from our measurements except for the covariance term ~~$\overline{w'|c'}$.~~ $\overline{|w|'c'}$. We define the "transport asymmetry coefficient" for the scalar c, (α_c) as the ratio of the covariance between the wind magnitude and the scalar to the covariance between the wind and the scalar.

$$\alpha_c = \frac{\overline{c'|w'|}}{\overline{c'w'}} = \frac{\rho_{c|w|}\sigma_{|w|}}{\rho_{cw}\sigma_w}$$

8

$$\alpha_c \equiv \frac{\overline{c'|w|'}}{\overline{c'w'}} \tag{12}$$

We notice α_c is conveniently independent of the scalar standard deviation. It can be written as

$$\alpha_c = \frac{\rho_{c|w|}\sigma_{|w|}}{\rho_{cw}\sigma_w} \tag{13}$$

where $\rho_{c|w|}$, ρ_{cw} are the correlation coefficients between c and $|w|$, and c and w, respectively. $\sigma_{|w|}$ and σ_w are the standard deviations of $|w|$ and w, respectively. After substitution, we write the turbulent flux as

$$\overline{w'c'} = \overline{wc} - \frac{\bar{w}}{\overline{|w|}}\,\overline{|w|c} + \frac{\bar{w}}{\overline{|w|}}\,\alpha_c\,\overline{w'c'} \tag{14}$$

Finally, we rearrange Eq. (14) and obtain the generalized TEA flux equation that gives a ~~correct~~ turbulent TEA flux when the mean vertical wind velocity is nonzero

$$\overline{w'c'} = \frac{\overline{wc}\,\overline{|w|} - \overline{|w|c}\,\bar{w}}{\overline{|w|} - \alpha_c\bar{w}} \tag{15}$$

2.4.1 ~~Values of transport asymmetry coefficient α_c~~ Calculating the corrected TEA flux

~~Calculating the correct flux using the new TEA equation~~

The new general equation for TEA (Eq. ~~(15))~~ ~~requires the knowledge of the transport asymmetry coefficient (α_c). An analytical expression for the value of α can be obtained from the knowledge of the joint probability distribution of the vertical wind velocity and the scalar. If the wind and the scalar are assumed to follow a Gaussian joint probability density function in the form~~

$$
\begin{aligned}
f(w,c) = {}& \frac{1}{2\pi\,\sigma_w\sigma_c\sqrt{1-\rho^2}} \times \\
& \exp\Bigg\{ -\frac{1}{2(1-\rho^2)}\Bigg(\frac{(w-\bar{w})^2}{\sigma_w{}^2} + \frac{(c-\bar{c})^2}{\sigma_c{}^2} \\
& \qquad\qquad -2\,\frac{\rho\,(w-\bar{w})\,(c-\bar{c})}{\sigma_w\sigma_c}\Bigg)\Bigg\}
\end{aligned}
$$

~~where ρ is the correlation coefficient between the~~ 15) extends the validity of the method to conditions where the mean vertical wind velocity ~~w and the scalar concentration c.~~

9

235 ~~We can express the analytical value of α_c in terms of the moments of the joint probability density function. We evaluate~~ is nonzero. We show here how the turbulent TEA flux can be calculated from the measured physical quantities.

$$\alpha_c = \frac{\overline{c'|w'|}}{\overline{c'w'}} = \frac{\overline{|w|\,c} - \overline{|w|}\,\bar{c}}{\overline{wc} - \bar{w}\,\bar{c}}$$

~~The term $\overline{|w|c}$ is obtained using~~ The weighted mean over an averaging period Δt can be written as

$$\overline{|w|\,c} = \int_{-\infty}^{\infty} \int_{-\infty}^{\infty} |w|\,c\,f(w,c)\,\mathrm{d}c\,\mathrm{d}w$$

240

$$\frac{\overline{c|w|}}{\overline{|w|}} = \overline{c|w\uparrow|}\,\frac{\overline{|w\uparrow|\Delta t^{\uparrow}}}{\overline{|w|\Delta t}} + \overline{c|w\downarrow|}\,\frac{\overline{|w\downarrow|\Delta t^{\downarrow}}}{\overline{|w|\Delta t}} \tag{16}$$

~~Accordingly, the term $\overline{wc}$ can be obtained as follows~~ which in terms of the quantities we are measuring, translates to

$$\overline{w\,c} = \int_{-\infty}^{\infty} \int_{-\infty}^{\infty} w\,c\,f(w,c)\,\mathrm{d}c\,\mathrm{d}w$$

245 $$\overline{c|w|} = \overline{|w|}\,\left(\frac{C_{acc}^{\uparrow} V^{\uparrow} + C_{acc}^{\downarrow} V^{\downarrow}}{V_{\text{total}}} \right) \tag{17}$$

~~After solving the integrals in Eq. (??) and Eq. (??) and substituting in Eq. (??), we find the value of α_c can be written using the mean vertical wind velocity and standard deviation as~~ Similarly

$$\alpha_c = \mathrm{erf}\left(\frac{\bar{w}}{\sqrt{2}\,\sigma_w} \right)$$

250 $$\overline{cw} = \overline{|w|}\,\left(\frac{C_{acc}^{\uparrow} V^{\uparrow} - C_{acc}^{\downarrow} V^{\downarrow}}{V_{\text{total}}} \right) \tag{18}$$

~~where erf is the error function. Therefore, the error in the flux when when failing to account for the correlation between the scalar and the magnitude of vertical wind velocity will lead to a flux biased by the last term of Eq. (14) $\bar{w}/\overline{|w|}\alpha_c$. We can further substitute the expected value of $|w|$ by the mean of~~

After substitution and simplification, we obtain the TEA flux in terms of ~~the folded normal distribution (Leone et al., 1961) and obtain an analytical expression for the expectation of the flux error due to a nonzero vertical wind velocity~~ measured quantities

$$F_{\mathrm{err}} = \overline{w}\pi \left(\cdot 2\sigma_w \mathrm{e}^{-\frac{(\overline{w})^2}{2\sigma_w{}^2}} + \mathrm{erf}\left(\cdot \frac{\overline{w}}{\sqrt{2}\,\sigma_w} \right) \overline{w}\pi \right)^{-1} \alpha_c$$

$$F_{\mathrm{TEA}} = \frac{C_{acc}^{\uparrow} V^{\uparrow}\left(\overline{|w|} - \bar{w}\right) - C_{acc}^{\downarrow} V^{\downarrow}\left(\overline{|w|} + \bar{w}\right)}{\overline{|w|} - \alpha_c \bar{w}} \times \frac{\overline{|w|}}{V_{total}} \tag{19}$$

~~Experimental evidence has shown that different scalars behave similarly (Ohtaki, 1985; Wesely, 1988). We expect the value of α to be similar for different scalars due to the similar transfer mechanism. Therefore, an empirical approach for estimating α for one scalar is to use α value from another available scalar, e. g. sonic temperature.~~

~~We can express the value of α in terms of the updraft and downdraft contributions to the flux (flux↑~~ Where F_{TEA} is the kinematic flux density $(\mathrm{mol\,m\,s^{-1}})$, $C_{acc}^{\uparrow}$ and ~~flux↓) as the difference of~~ $C_{acc}^{\downarrow}$ are the mean concentrations $(\mathrm{mol\,m^{-3}})$ of the scalar c in updraft and downdraft reservoirs at the end of the averaging period, Δt. $V^{\uparrow}$ and $V^{\downarrow}$ are the accumulated sample volumes $(\mathrm{m^3})$ in updraft and downdraft ~~fluxes to the total flux.~~

~~α_c can be written to a good approximation as~~

$$\alpha_c = \frac{\mathrm{flux}^{\uparrow} - \mathrm{flux}^{\downarrow}}{\mathrm{flux}^{\uparrow} + \mathrm{flux}^{\downarrow}}$$

~~where the updraft and the downdraft contributions to the flux (flux$^{\uparrow}$, and flux$^{\downarrow}$) are defined as~~

$$\mathrm{flux}^{\uparrow} = \overline{c'^{\uparrow}w'^{\uparrow}}\,\mathrm{P}(w^{\uparrow})$$

$$\mathrm{flux}^{\downarrow} = \overline{c'^{\downarrow}w'^{\downarrow}}\,\mathrm{P}(w^{\downarrow})$$

~~where P$(w^{\uparrow})$ is the probability of a vertical wind velocity with a positive direction, P$(w^{\downarrow})$ is the probability of a~~ reservoirs during the averaging period. $\overline{|w|}$ is the mean of the absolute vertical wind velocity ~~with a negative direction.~~ $(\mathrm{m\,s^{-1}})$ during the averaging period.

11

2.5 Values of the transport asymmetry coefficient α_c

2.5.1 Quadrant analysis of α_c

The ~~expression of α in terms of updraft and downdraft flux contributions is closely related to~~ value of α_c can be analyzed using the framework of quadrant analysis. ~~We include it here for completeness.~~ Quadrant analysis is commonly used to inspect the contributions from different quadrants in the (w', c') plane by sorting the instantaneous values into four categories $(S_1 .. S_4)$ according to the sign of the two fluctuating components (e.g., (Katul et al., 1997; Raupach, 1981; Katsouvas et al., 2007). ~~We find that α can be written in terms of quadrants as~~

$$\alpha = \frac{S_1 + S_4 - (S_2 + S_3)}{S_1 + S_2 + S_3 + S_4}$$

). Where S_i is the fraction of the flux transported by contributions in quadrant i ~~, given as~~

$$S_i = \frac{\langle\langle w'c'\rangle\rangle_i}{\overline{w'c'}}$$

~~$\langle\langle wc \rangle\rangle_i$ is the conditional average defined as~~

$$\langle\langle wc \rangle\rangle_i = \lim_{T \to \infty} \frac{1}{T_p} \int_0^{T_p} w'(t)c'(t)I_i \mathrm{d}t$$

~~The indicator function I_i obeys~~

$$I_i(w', c') = \begin{cases} 1, & \text{if } (w', c') \text{ in quadrant } i \\ 0, & \text{otherwise} \end{cases}$$

. Following the definition of Thomas and Foken (2007), the pairs S_2 and S_4 are ejections and sweeps for downward directed net flux (negative ρ_{wc}) and S_1 and S_3 for upward directed net flux (positive ρ_{wc}).

2.5.2 ~~Calculating the corrected TEA flux~~

~~The new general equation for TEA (Eq. 15) extends the validity of the method to conditions where the mean vertical wind velocity is nonzero. We show here how the correct TEA flux can be calculated from the measured physical quantities.~~

~~The weighted mean over an averaging period T_{avg} can be~~ The total flux is the sum of the contributions from the four quadrants, we similarly find that the covariance term $\overline{|w'|c'}$ can be written as

$$\frac{\overline{c|w|}}{\overline{|w|}} = \overline{c|w\uparrow|} \frac{\overline{|w\uparrow|T^\uparrow_{avg}}}{\overline{|w|T_{avg}}} + \overline{c|w\downarrow|} \frac{\overline{|w\downarrow|T^\downarrow_{avg}}}{\overline{|w|T_{avg}}}$$

$$\overline{|w'|c'} = S_1 + S_4 - S_2 - S_3 \tag{20}$$

~~which~~ It follows that α can be written in terms of ~~the quantities we are measuring, translates to~~ quadrants as

300 $$\overline{c|w|} = \overline{|w|} \left(\frac{C^\uparrow_{acc} V^\uparrow + C^\downarrow_{acc} V^\downarrow}{V_{\text{total}}} \right)$$

$$\alpha = \frac{S_1 + S_4 - (S_2 + S_3)}{S_1 + S_2 + S_3 + S_4} \tag{21}$$

~~Similarly~~

$$\overline{cw} = \overline{|w|} \left(\frac{C^\uparrow_{acc} V^\uparrow - C^\downarrow_{acc} V^\downarrow}{V_{\text{total}}} \right)$$

305 It should be noted that when $\bar{w} \neq 0$, $\overline{|w'|c'}$ is an approximation for $\overline{|w|'c'}$, the latter can be found to be

$$\overline{|w|'c'} = \overline{|w' + \bar{w}|'c'} \tag{22}$$

~~After substitution and simplification, we obtain the correct TEA flux in terms of the measured quantities~~ The contributions of $\overline{|w|'c'}$ can be accommodated in this analysis by partitioning the contributions into six categories, the four quadrants and two additional bands for the contributions when w' falls between 0 and $\bar{w}$. However, the contribution from the additional bands is 310 small and has little impact on the interpretation of this analysis.

$$F_{\text{TEA}} = \frac{C^\uparrow_{acc} V^\uparrow \left(\overline{|w|} - \bar{w} \right) - C^\downarrow_{acc} V^\downarrow \left(\overline{|w|} + \bar{w} \right)}{\overline{|w|} - \alpha_c \bar{w}} \times \frac{\overline{|w|}}{V_{total}}$$

Considering that the quadrants $S1$ and $S4$ represent the contribution of updrafts to the flux. Similarly, $S2$ and $S3$ represent the contribution of downdrafts to the flux. We define

$$\text{flux}^\uparrow = S1 + S4 \tag{23}$$

315 $$\text{flux}^\downarrow = S2 + S3 \tag{24}$$

Where F_{TEA} is the kinematic flux density (). $C_{acc}^{\uparrow}$ and $C_{acc}^{\downarrow}$ are the mean concentrations () of the scalar c in updraft and downdraft reservoirs at the end of Here, the accumulation averaging period T_{avg}. arrows indicate the direction of the wind and not the sign of the flux. e.g., flux$^{\uparrow}$ is the portion of the flux transported with updrafts which can be either positive or negative flux. $V^{\uparrow}$ and $V^{\downarrow}$ are the accumulated sample volume () in updraft and downdraft reservoirs at the end of the averaging period.

320 If follows that α_c can be written as

$$\alpha_c = \frac{\text{flux}^{\uparrow} - \text{flux}^{\downarrow}}{\text{flux}^{\uparrow} + \text{flux}^{\downarrow}} \tag{25}$$

The previous equation indicates that if the flux transported with updrafts, flux$^{\uparrow}$ have the same sign as the flux transported with downdrafts, flux$^{\downarrow}$, then the value of $|\alpha_c|$ will be smaller than one. If $|\alpha_c| > 1$ then flux$^{\uparrow}$ and flux$^{\downarrow}$ have opposing signs which indicates that the wind and the scalar are correlated for updrafts and anti-correlated for downdrafts or vice versa, indicating

325 non-stationary conditions.

2.5.2 Analytical value of α_c

An analytical expression for the value of α can be obtained from the knowledge of the joint probability distribution of the vertical wind velocity and the scalar. If the wind and the scalar are assumed to follow a Gaussian joint probability density function, $\overline{|w|}$ is the we find the analytical value of α_c in terms of the moments of the joint probability density function to be

330 $$\alpha_c = \mathrm{erf}\left(\frac{\bar{w}}{\sqrt{2}\,\sigma_w}\right) \tag{26}$$

Where erf is the error function. σ_w is the wind standard deviation.

We can use the analytical value of α_c and further substitute the expected value of $|w|$ with the mean of the absolute folded normal distribution (Leone et al., 1961) to obtain an analytical expression for the expectation of the flux error due to a nonzero vertical wind velocity () during the averaging period. $\bar{w}$ is the mean of the using $\bar{w}$ and σ_w. By substituting into the last term of

335 Eq. (14), $\bar{w}/\overline{|w|}\alpha_c$

$$F_{\mathrm{err}} = \overline{w}\pi \left(2\sigma_w e^{-\frac{(\overline{w})^2}{2\,\sigma_w{}^2}} + \mathrm{erf}\left(\frac{\overline{w}}{\sqrt{2}\,\sigma_w}\right) \overline{w}\pi \right)^{-1} \alpha_c \tag{27}$$

Here, F_{err} is the error in the TEA flux when failing to account for the correlation between the scalar and the magnitude of vertical wind velocity.

2.5.3 Scalar similarity to estimate α_c

14

340 The assumption of scalar similarity provides a potential empirical way to estimate the value of α_c ~~is the transport asymmetry coefficient for the scalar c (dimensionless).~~, i.e., by calculating the value of α_c from another scalar where high-frequency measurements are available, e.g. sonic temperature. The assumption of scalar similarity is supported by experimental evidence that has shown that different scalars behave similarly due to a similar transfer mechanism (Ohtaki, 1985; Wesely, 1988). However, the assumption of scalar similarity can not be always guaranteed and should be used with caution. Nonetheless,

345 we believe it is a useful assumption to approximate the value of α_c given that the value of α_c is determined by the distribution of turbulent transport in different quadrants which is expected to have the same effect on different scalars under good mixing conditions.

3 Methods

3.1 Numerical simulations

350 ~~In addition to the experiment described earlier, we~~ We set up a numerical simulation to test the magnitude of the error due to nonzero $\bar{w}$ on the flux ~~. We used high-frequency~~ and investigate the values of the coefficient α_c. For this simulation, we used 10 Hz measurements obtained from ~~the IRGAand the sonic anemometerduring one week from 19~~ a field experiment measuring vertical wind velocity and scalar concentration using an infrared gas analyzer (IRGA) and a sonic anemometer. We used data from a period of 12 days from 15 June 2020 to 26 June 2020. The data were collected at an ideal flat agricultural

355 site in Braunschweig, Germany. A full description of the site and the instrumentation are provided in the accompanying paper (Emad and Siebicke, 2022). We added a random $\bar{w}$ offset in the range (-0.25 to $0.25 \mathrm{~m~s}^{-1}$) to each averaging interval but limited $\bar{w}$ to smaller than $2\sigma_w$. We obtained ~~6~~ 3 repetitions and calculated the flux according to different formulas. In total, there were about ~~1800~~ 1400 30-minute averaging intervals. The methods compared were: i) the flux calculated using the concentrations formula of Hicks and McMillen (1984) shown in Eq. (8), ii) the equation for DEA including the non equal

360 volume correction of Turnipseed et al. (2009), and iii) the new generalized equation proposed in the current study (Eq. 14) utilizing α_θ values calculated from sonic temperature and the analytical value of α_c.

We applied minimal quality checks on the resulting fluxes before the comparison. ~~We applied the steady state test following Foken et al. (2005) , which removed 24%~~ Tests for stationarity following Foken et al. (2005) removed 22% of the averaging intervals. We limited the values of $|\alpha_\theta|$ to less than ~~0.7~~ 1, which removed an additional ~~11%~~ 4% of the averaging intervals.

365 Furthermore, when the sonic temperature was used for calculating α_θ, periods with low turbulence intensity, $|\rho_{w\theta}| < 0.2$ where excluded. The excluded averaging intervals occurred almost exclusively during ~~low developed turbulence and~~ night-time conditions.

4 Results and Discussion

We first discuss the ~~problem of nonzero mean vertical wind velocity and the new generalized TEA equation~~ newly proposed

370 TEA equation, then compare it to different TEA formulations. Then, we discuss the ~~value and~~ interpretation of the transport

asymmetry coefficient α ~~. Next, we discuss the newly proposed short-time eddy accumulation method. Then, we discuss some results and aspects of the STEA flux calculations. Afterwards, we will present the flux intercomparison between STEA and EC. Finally, we discuss the effect of using fixed buffer volumes on the fluxes and the proposed empirical correction.~~ and different ways of estimating it.

4.1 Nonzero mean vertical wind velocity

~~We presented a new formulation for the TEA equation . The new equation~~ The newly proposed TEA equation (Eq. (14)) successfully constrained the biased advective term $\overline{w}\bar{c}$. The new equation employs information about the scalar transport to allow the estimation of $\bar{c}$ from available TEA measurements and, consequently ~~, constraining the bias term $\overline{w}\bar{c}$~~ get an estimate of the biased advective term. Besides the correction of the nonzero $\overline{w}$ bias, the estimation of the scalar mean, $\bar{c}$ is essential for the WPL correction and the calculation of storage fluxes.

The terms of Eq. 14 account for different contributions to the flux. The first term on the ~~right hand~~ right-hand side is equivalent to calculating the flux as the difference in accumulated mass between updraft and downdraft. When $\bar{w} = 0$, the equation is reduced to this term only. The second term accounts for the bias introduced by the biased advective term $\bar{w}\bar{c}$ by using the weighted mean of the scalar and the magnitude of wind as an estimate for $\bar{c}$. We show that when $\bar{w} \neq 0$, the first two terms are equivalent to using the concentration formula of Hicks and McMillen (1984) shown in Eq. (8), with the unequal volume correction of Turnipseed et al. (2009) that accounts for the small difference between the weighted mean $\bar{c}_{\mathrm{W}}$ and average of concentrations $(C_{acc}^{\uparrow} + C_{acc}^{\downarrow})/2$. Refer to appendix A for details about this equality. The new third term ~~$\overline{c'|w'|}/|w|$~~ $\overline{c'|w|'}/\overline{|w|}$ corrects for the correlation between the scalar and the magnitude of the wind. Ignoring the third term will result in a flux biased with the ratio $\bar{w}/\overline{|w|}\alpha_c$.

The new TEA equation reveals an important insight. When using the new equation to calculate the flux, the error in the flux when $\overline{w} \neq 0$ is independent of the scalar concentration and is governed by the characteristics of the turbulent transport. This ~~gives higher~~ strengthens the confidence in using the TEA method for measuring atmospheric constituents with high background concentration and small flux (low deposition velocity).

Using the new TEA formula with an estimated value for α_c was effective in reducing the uncertainty and the systematic error in the calculated fluxes (Fig. 1). To quantify the ~~effect of nonzero $\overline{w}$~~ magnitude of the systematic bias and uncertainty resulting from nonzero $\bar{w}$ on the fluxes, we used the ~~results of the numerical simulation explained in the methods section. The results of the comparison are presented in Fig. 1. Additionally, we used the~~ simulation results to obtain the slope and the coefficient of determination, R^2 ~~obtained~~ from a linear fit of the calculated fluxes against the reference EC flux~~and the mean absolute difference, MAD to compare the different formulations.~~. The simulation results show an increased bias and uncertainty in the fluxes when $\bar{w} \neq 0$ and a significant improvement when using an estimate of α for correction (Fig. 1).

~~a) Comparison of different equations of TEA flux calculation against a reference EC flux. Data were obtained from a numerical simulation using high frequency measurements over a one-week period from 19 June 2020 to 26 June 2020. We added a random $\bar{w}$ offset in the range (-0.25 to 0.25)). Colors represent different formulas. b) Kernel density estimates of the flux error ratio using the three different formulas.~~
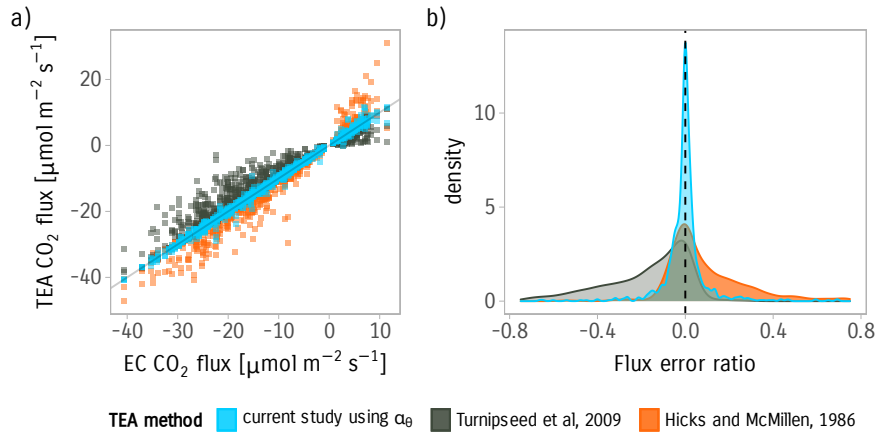
Figure 1. a) Comparison of different equations of TEA flux calculation against a reference EC flux. Data were obtained from high frequency measurements over 12 days from 15 June 2020 to 26 June 2020 and included an added random $\bar{w}$ offset in the range (-0.25 to 0.25 $\mathrm{m\,s^{-1}}$)). Colors represent different formulas. b) Kernel density estimates of the flux error ratio using the three different formulas.

405   We found that ~~by ignoring the correction completely and using the~~ using the accumulated mass difference to calculate the TEA flux (first term in Eq. 14) produced the largest errors. Values of $\bar{w}$ as small as $0.01\,\sigma_w$ was sufficient to produce more than 10% mean bias in the flux magnitude for CO_2 in our dataset.

     The use of the concentration TEA equation of Hicks and McMillen (1984) ~~, the TEA flux was overestimated~~ was a considerable improvement over using the mass difference but still overestimated the TEA flux. The slope of the linear fit was ~~1.09 ($R^2 = 0.96$)and~~

410 ~~the mean absolute difference (MAD) was 0.97 .~~ $1.12\ (R^2 = 0.94)$. Using the DEA equation of Turnipseed et al. (2009) which includes an additional term to correct for the effect of unequal volume on the flux, ~~the linear fit slope was 0.88 ($R^2 = 0.95$)and~~ ~~the mean absolute difference was MAD = 1.03 .~~ led to underestimating the TEA flux yielding a slope of $0.84\ (R^2 = 0.93)$. The correction of nonzero $\bar{w}$ using α_θ ~~significantly improved the match. The linear fit produced a slope of almost 1 ($R^2 = 0.997$).~~ ~~The mean absolute difference was 0.26 almost four times smaller than the other two methods.~~ utilizing the assumption of scalar

415 similarity significantly reduced the bias and the uncertainty and gave slope of $1.005\ (R^2 = 0.995)$. The use of the analytical value of α_c using Eq. 26 similarly reduced the bias but with a smaller reduction in uncertainty, yielding a slope of 0.991 $(R^2 = 0.97)$.

     These results indicate that the proposed ~~correction significantly reduces the bias and uncertainty of TEA fluxes~~ corrections using an estimate of α_c are very effective in minimizing or removing the bias from TEA flux when $\bar{w} \neq 0$ even when using the

420 analytical value of α_c.

4.1.1 ~~Value and interpretation of the transport asymmetry coefficient α~~

4.2 Value and interpretation of the transport asymmetry coefficient α

17
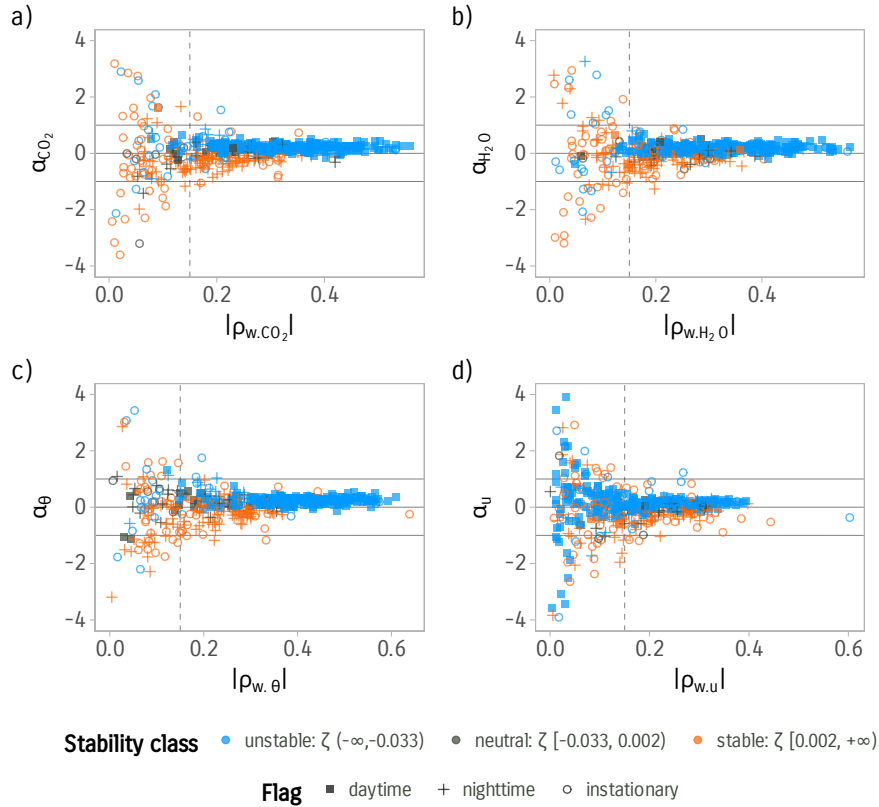
Figure 2. Observed values of the transport asymmetry coefficient α vs. the correlation coefficient for four variables calculated from hight-frequency measurements. a) CO_2, b) H_2O, c) sonic temperature, θ, and d) wind velocity component, u. Colors distinguish different stability classes. Point shape differentiates daytime, nighttime, and instationary conditions following Foken and Wichura (1996). Vertical dashed line is set to $x = 0.15$ and the horizontal lines are set to $y = -1$ and $y = 1$.

~~We proposed the transport asymmetry coefficient~~

The value of α_c ~~,~~ defined in Eq. (12) ~~as the ratio between the covariance of the scalar and the absolute value of vertical~~
425 ~~wind $\overline{|w'|c'}$ to the covariance between the scalar and the vertical wind $\overline{w'c'}$. The value of α_c~~ indicates the disparity of the flux transport between updrafts and downdrafts. ~~We showed the analytical expectation of α based on the assumption of a joint Gaussian distribution in Eq. (??~~Values of α_c larger than 1 indicate that updraft flux $(S_1 + S_4)$ and downdraft flux $(S_2 + S_3)$ have opposing signs. This pattern indicates that the wind and the scalar are correlated for updraft flux and anti-correlated for the downdraft flux (or the other way around). This ~~assumption, although used in the literature e. g. (Wyngaard and Moeng, 1992),~~
430 ~~is not adequate. While the wind might be normally distributed for most stability classes (Chu et al., 1996),~~ pattern violates the stationarity conditions.

18

Therefore, we conclude that for stationary flows the systematic error in the TEA flux is smaller than $\pm \bar{w}/\overline{|w|}$. Observed values of α for H_2O, CO_2, θ, and the wind component, u are shown in Fig. 2. The data confirm that values of $|\alpha|$ are consistently below 1 for the ~~scalar can depart significantly from normality (Berg and Stull, 2004).Other distributions might be more suited~~

435   ~~for approximating the joint probability distribution (Frenkiel and Klebanoff, 1973). For example, Katsouvas et al. (2007) showed using experimental data that a third-order Gram–Charlier distribution was necessary and sufficient in most of the cases for describing the quadrant time and flux contributions.~~ four scalars when the stationarity criterion is met. However, when the correlation between w and the scalar is low during conditions associated with low developed turbulence, spurious correlations might lead to values of $|\alpha|$ larger than one.

440   We found ~~using high-frequency measurements~~ that the value of α for CO_2 correlates moderately with the skewness of the measured scalar ($r = 0.61$~~). On average, updrafts have larger contribution to the flux. The~~, data not shown). The observed mean of α for CO_2 and sonic temperature calculated from high-frequency measurements for periods with negligible $\bar{w}$ was approximately 0.2 ~~under~~ for unstable and good turbulent mixing conditions ($|\rho_{wc}| > 0.25$) with a standard error, $SE = 0.01$. ~~Under~~ For stable stratification ($\zeta > 0$), the mean of α was approximately equal to -0.18 but with a higher spread around

445   the mean, $SE = 0.09$. ~~These values~~ These values indicate that updrafts have larger contribution to the flux under unstable stratification and smaller contribution during stable stratification. The results generally agree with values found from studies using conditional sampling (Greenhut and Khalsa, 1982) and LES simulations (Wyngaard and Moeng, 1992) which found that updrafts contribution to the flux is 2 to 3 times larger than downdrafts under unstable conditions due to the contribution of convective thermals.

450   The sign of α indicate whether updrafts or downdrafts have a larger contribution to the flux. Inspecting Eq. 25, we find that a positive α indicate that the magnitude of updrafts contribution to the flux is larger than the magnitude of the downdrafts contribution, $|\mathrm{flux}^{\uparrow}| > |\mathrm{flux}^{\downarrow}|$ while the opposite is true for a negative α.

~~We showed that~~ The analytical value of α from Eq. (26) was effective in minimizing the systematic bias as confirmed by the simulation results. However, the assumption of a Gaussian distribution, although used in the literature, e.g., (Wyngaard and Moeng, 1992)

455   , is not adequate. While the wind might be normally distributed for most stability classes (Chu et al., 1996), the ~~bias in TEA flux when $\bar{w} \neq 0$ is dependent on the value of α_c.For TEA, α_c is not readily available, since its calculation requires the high-frequency information of the scalar . Similarity of scalar transport suggests that~~ scalar can depart significantly from normality (Berg and Stull, 2004). Other distributions might be more suited for approximating the joint probability distribution (Frenkiel and Klebanoff, 1973). For example, Katsouvas et al. (2007), using experimental data, showed that a third-order Gram–Charlier

460   distribution was necessary and sufficient in most of the cases for describing the quadrant time and flux contributions. It is worth considering this distribution to find a better analytical formula to calculate the expectation of α ~~values for different scalars should be similar, allowing the use of α_θ calculated from sonic temperature as a substitute for α_c.~~.

The hypothesis of scalar similarity was proposed as another source for estimating the values of α. The similarity was confirmed empirically by ~~calculating~~ investigating the values of α_θ and α_c from high-frequency measurements ~~.~~ (Fig. 3). A

465   linear fit with a slope of 0.98 and R^2 of ~~0.962~~ 0.92 was obtained during steady-state and well-developed turbulence conditions. During such conditions, α_θ can substitute α_c to calculate the flux correction ratio. However, the correction becomes large

19
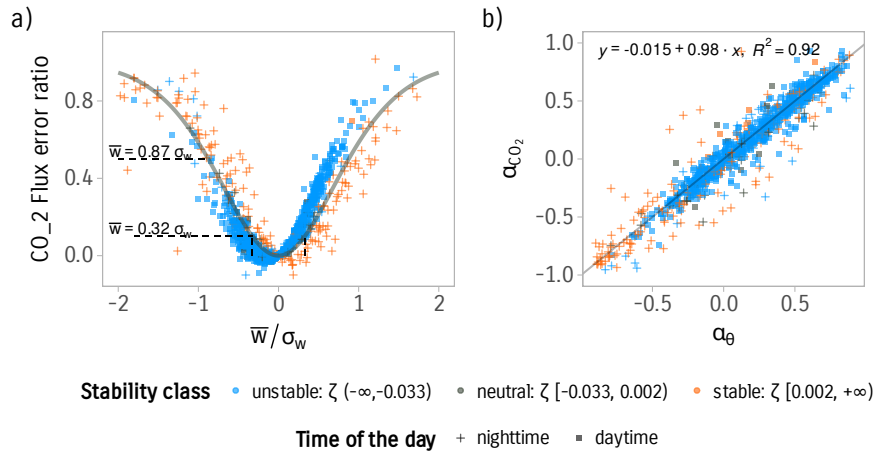
Figure 3. a) The error ratio in the CO_2 flux calculated using the TEA method due to nonzero mean vertical wind. The solid gray line represents the analytical values of the error in the flux (if a joint Gaussian probability distribution is assumed). The points are the observed error calculated from high-frequency measurements colored according to stability classes. The point shape distinguishes day-time and night-time data. b) Relation of α_{CO_2} calculated for CO_2 and α_θ calculated from sonic temperature and a 1-to-1 line for reference.

and unreliable in periods where σ_w and ρ_{cw} are small, associated with small fluxes during night-time and stable conditions. Additionally, temperature is considered a bad proxy during near-neutral conditions ~~(McBean, 1973; Hicks et al., 1980)~~ due to its contribution to buoyancy (McBean, 1973; Hicks et al., 1980). We noticed that the variance in α values is higher under

470   weakly developed turbulence ~~. We~~ and experimentally determined the threshold for the ~~safe use of α for~~ optimum use of α_θ ~~for the~~ correction as $|\rho_{cw}| = 0.2$. Below this threshold, values of ~~α larger than 0.5~~ α_θ larger than 1 are observed, making the correction unreliable. This threshold can be seen as an indicator for the violation of assumptions of homogeneity and stationarity or other problematic conditions. Similar uses for the correlation coefficient are common in the literature e.g. (Foken and Wichura, 1996).

475   ~~a) The error ratio in the flux calculated using the TEA method due to nonzero mean vertical wind. The solid gray line represents the analytical values of the error in the flux (if a joint Gaussian probability distribution is assumed). The points are the observed error calculated from high-frequency measurements colored according to stability classes. The point shape distinguishes day-time and night-time data. b) Relation of α_{CO_2} calculated for and and α_θ calculated from sonic temperature and a 1-to-1 line for reference.~~

480   ~~We determined~~ Another use of the formulation using α is to find a $\bar{w}$ threshold, above which, the TEA flux measurement becomes unreliable. For example, if we define that the bias in the flux should not exceed 10% of the flux, we can find experimentally that the error in the flux due to nonzero $\bar{w}$ becomes ~~significant (~~larger than 10% ~~of the flux)~~ when $\bar{w}$ exceeds $0.21\sigma_w$ for periods with good turbulent mixing conditions ($|\rho_{w,CO_2}| > 0.2$). This threshold is close to the analytical value of $0.323\,\sigma_w$ obtained from the Gaussian joint probability distribution. To push this threshold further, α_θ calculated from sonic temperature

can be used during good turbulent mixing conditions ($|\rho_{w,CO_2}| > 0.2$). Simulations indicate that the average relative confidence interval for the predicted value of α_θ from α_{CO_2} is 0.17% of the fit value. ~~In summary~~In summary for this example, to keep the error in the flux below 10%, α_θ can be safely used to correct for biased $\bar{w}$ as long as $\bar{w} < 0.7\,\sigma_w$. This limit is considered forgiving and easy to achieve with online coordinates rotation and ~~other~~ further rather simple online treatments. The only times where this limit is expected to be reached is when σ_w is very small (e.g., during night-time conditions) where other problems such as low ~~turbulence~~ turbulent mixing and violations of the ~~method's assumptions~~ assumptions of the EC and TEA methods are expected to occur. These periods largely overlap with periods considered of low quality and are usually excluded from the analysis (Foken et al., 2012b).

To summarize, we find that the error in the TEA flux is constrained to $\bar{w}/\overline{|w|}$ for $|a| < 1$, which was shown here to be true for stationary conditions, which are at the focus of turbulent flux measurements. If a correction is desired to minimize this error, two options were presented to estimate α_c: first, an analytical solution, and second, an estimate employing scalar similarity. Finally, with the use of α_c, the typically observed systematic flux bias due to nonzero mean vertical wind velocity could be effectively characterized and minimized.

5 Conclusions

In this paper, we revised the theory of the true eddy accumulation method and extended the applicability of the method to measure the turbulent flux under non-ideal conditions where the mean vertical wind velocity during the averaging interval is not zero. The new generalized equation allows estimating the scalar mean during the flux averaging interval and ~~define~~ defining conditions where the error in the flux is significant. We found that the error in the TEA flux is a function of the disparity of atmospheric transport and defined ways and conditions to constrain that error. We found that it is possible to achieve minimum bias in the TEA flux under most atmospheric conditions as well as identify those conditions which are less favorable. We believe that these results increase the confidence in using the TEA method for different atmospheric constituents and under a variety of atmospheric conditions.

~~Additionally, we proposed an alternative method for the measurement of ecosystem-level fluxes. The new method, referred to as short-time eddy accumulation (STEA), allows the sample accumulation to be carried out on shorter varying-length intervals. The method offers more flexibility than TEA and has many potential benefits including a better dynamic range and higher accuracy than the TEA method, and the ability to operate under a flow-through scheme using fixed buffer volumes. The flexibility introduced by the new method offers new ways to design eddy accumulation systems particularly suited for a specific atmospheric constituent or a specific gas analyzer. For example, the accumulation time can be tailored to measure reactive species or to distribute the gas analyzer time to measure the fluxes at different heights.~~

~~Furthermore, we presented a prototype evaluation of the STEA method under the flow-through regime. We described the details of the system design and operation. We compared flux measurements from our new system against a reference EC system over a flat agricultural field. The fluxes from the two methods were in very good agreement. We highlighted the importance of different processing and design aspects between the two methods and their potential effect on the fluxes.~~

520

Code and data availability. All data needed for producing the figures presented in the paper are provided at Emad and Siebicke (2021b). Scripts for producing the plots in the paper are available at Emad and Siebicke (2021a). Currently, drafts are accesible at: https://s.gwdg.de/

525 R4Fdhg and https://s.gwdg.de/CZ4zXI.

Appendix A: Hicks and McMillen formulation

We show here how the TEA flux formula of Hicks and McMillen (1984), originally formulated under the assumption of $\bar{w} = 0$ is equivalent to using $(C_{acc}^{\uparrow} + C_{acc}^{\downarrow})/2$ as an estimate for $\bar{c}$ in the second term on the right hand side of Eq. (2).

We write the conditional expectation of $\bar{w}$ as

530 $$\bar{w} = \overline{\left(\overline{w|\text{sign}(w)}\right)} = \overline{|w^{\uparrow}|}\, \text{P}(w^{\uparrow}) - \overline{|w^{\downarrow}|}\, \text{P}(w^{\downarrow}) \tag{A1}$$

where $\text{sign}(w)$ is the sign of vertical wind velocity. $\text{P}(w^{\uparrow})$ and $\text{P}(w^{\downarrow})$ are the observed probabilities of the sign of w, which equals the ratio of the time the wind is positive or negative to the total integration interval time.

$$\bar{w} = \overline{|w^{\uparrow}|}\frac{T_{avg}^{\uparrow}}{T_{avg}} - \overline{|w^{\downarrow}|}\frac{T_{avg}^{\downarrow}}{T_{avg}}$$

535 $$\bar{w} = \overline{|w^{\uparrow}|}\frac{\Delta t^{\uparrow}}{\Delta t} - \overline{|w^{\downarrow}|}\frac{\Delta t^{\downarrow}}{\Delta t} \tag{A2}$$

and similarly

$$\overline{|w|} = \overline{|w^{\uparrow}|}\frac{T_{avg}^{\uparrow}}{T_{avg}} + \overline{|w^{\downarrow}|}\frac{T_{avg}^{\downarrow}}{T_{avg}}$$

$$\overline{|w|} = \overline{|w^{\uparrow}|}\frac{\Delta t^{\uparrow}}{\Delta t} + \overline{|w^{\downarrow}|}\frac{\Delta t^{\downarrow}}{\Delta t} \tag{A3}$$

540 by substituting $\overline{|w|}/2$ with

22

$$\frac{\overline{|w|}}{2} = \overline{|w^\uparrow|}\frac{T_{avg}^\uparrow}{T_{avg}} - \frac{\bar{w}}{2} = \overline{|w^\downarrow|}\frac{T_{avg}^\downarrow}{T_{avg}} + \frac{\bar{w}}{2}$$

$$\frac{\overline{|w|}}{2} = \overline{|w^\uparrow|}\frac{\Delta t^\uparrow}{\Delta t} - \frac{\bar{w}}{2} = \overline{|w^\downarrow|}\frac{\Delta t^\downarrow}{\Delta t} + \frac{\bar{w}}{2} \tag{A4}$$

we obtain

$$C_{acc}^\uparrow(\overline{w^\uparrow}\,\frac{T_{avg}^\uparrow}{T_{avg}} - \frac{\bar{w}}{2}) - C_{acc}^\downarrow(\overline{|w^\downarrow|}\,\frac{T_{avg}^\downarrow}{T_{avg}} + \frac{\bar{w}}{2})$$

$$C_{acc}^\uparrow(\overline{w^\uparrow}\,\frac{\Delta t^\uparrow}{\Delta t} - \frac{\bar{w}}{2}) - C_{acc}^\downarrow(\overline{|w^\downarrow|}\,\frac{\Delta t^\downarrow}{\Delta t} + \frac{\bar{w}}{2}) \tag{A5}$$

After rearrangement and simplification we get to

$$F_{\text{EA}} = \overline{cw} - \bar{w}\left(\frac{C_{acc}^+ + C_{acc}^-}{2}\right) \tag{A6}$$

When Eq. (A6) is compared with Eq. (2), it is clear that the term $\frac{C_{acc}^+ + C_{acc}^-}{2}$ is used as an estimate for $\bar{c}$.

Appendix B: List of symbols

Table B1. Symbols and subscripts with units

Symbols

Symbol	Units	Description
c	$\mathrm{mol\,m^{-3}}$	Molar density of a scalar
w	$\mathrm{m\,s^{-1}}$	Vertical wind velocity
~~T_{avg}~~ Δt	s	Flux averaging interval
A	–	TEA sampling scaling factor
V	$\mathrm{m^3}$	Volume
C	$\mathrm{mol\,m^{-3}}$	Mean concentration of accumulated samples
α_c	–	Transport asymmetry coefficient for scalar c
ρ	–	~~Corelation~~ Correlation coefficient
~~$\dot{q}$~~ S_i	–	~~Dimensionless mass flow rate~~ Flux contribution from quadrant i

~~τ Time constant of the buffer volume~~

~~r_c Mixing ratio in dry air for a scalar, c~~**Subscripts**

Subscript	Description
acc	Accumulated samples
↑	Updraft buffer volume
↓	Downdraft buffer volume
c	Atmospheric constituent

References

Baldocchi, D.: Measuring Fluxes of Trace Gases and Energy between Ecosystems and the Atmosphere - the State and Future of the Eddy Covariance Method, Global Change Biology, 20, 3600–3609, https://doi.org/10.1111/gcb.12649, 2014.

Baldocchi, D. D., Hicks, B. B., and Meyers, T. P.: Measuring Biosphere-Atmosphere Exchanges of Biologically Related Gases with Micrometeorological Methods, Ecology, 69, 1331–1340, https://doi.org/10.2307/1941631, 1988.

Berg, L. K. and Stull, R. B.: Parameterization of Joint Frequency Distributions of Potential Temperature and Water Vapor Mixing Ratio in the Daytime Convective Boundary Layer, Journal of the Atmospheric Sciences, 61, 813–828, https://doi.org/10.1175/1520-0469(2004)061<0813:POJFDO>2.0.CO;2, 2004.

Bowling, D. R., Turnipseed, A. A., Delany, A. C., Baldocchi, D. D., Greenberg, J. P., and Monson, R. K.: The Use of Relaxed Eddy Accumulation to Measure Biosphere-Atmosphere Exchange of Isoprene and Other Biological Trace Gases, Oecologia, 116, 306–315, https://doi.org/10.1007/s004420050592, 1998.

Businger, J. A. and Oncley, S. P.: Flux Measurement with Conditional Sampling, Journal of Atmospheric and Oceanic Technology, 7, 349–352, https://doi.org/10.1175/1520-0426(1990)007<0349:FMWCS>2.0.CO;2, 1990.

Chu, C. R., Parlange, M. B., Katul, G. G., and Albertson, J. D.: Probability Density Functions of Turbulent Velocity and Temperature in the Atmospheric Surface Layer, Water Resources Research, 32, 1681–1688, https://doi.org/10.1029/96WR00287, 1996.

Desjardins, R. L.: Energy Budget by an Eddy Correlation Method, Journal of Applied Meteorology, 16, 248–250, https://doi.org/10.1175/1520-0450(1977)016<0248:EBBAEC>2.0.CO;2, 1977.

Emad, A. and Siebicke, L.: Replication Code for: Advances in the True Eddy Accumulation Method: New Theory, Implementation, and Field Results, https://doi.org/10.25625/SYQITK, 2021a.

Emad, A. and Siebicke, L.: Replication Data for: Advances in the True Eddy Accumulation Method: New Theory, Implementation, and Field Results, https://doi.org/10.25625/IVTS87, 2021b.

Emad, A. and Siebicke, L.: True Eddy Accumulation - Part 2: Theory and Experiment of the Short-Time Eddy Accumulation Method [Submitted along This Paper], Atmospheric Measurement Techniques Discussions, 2022.

Finnigan, J. J., Clement, R., Malhi, Y., Leuning, R., and Cleugh, H.: A Re-Evaluation of Long-Term Flux Measurement Techniques Part I: Averaging and Coordinate Rotation, Boundary-Layer Meteorology, 107, 1–48, https://doi.org/10.1023/A:1021554900225, 2003.

Foken, T. and Wichura, B.: Tools for Quality Assessment of Surface-Based Flux Measurements, Agricultural and Forest Meteorology, 78, 83–105, https://doi.org/10.1016/0168-1923(95)02248-1, 1996.

Foken, T., Göockede, M., Mauder, M., Mahrt, L., Amiro, B., and Munger, W.: Post-Field Data Quality Control, in: Handbook of Micrometeorology: A Guide for Surface Flux Measurement and Analysis, edited by Lee, X., Massman, W., and Law, B., Atmospheric and Oceanographic Sciences Library, pp. 181–208, Springer Netherlands, Dordrecht, https://doi.org/10.1007/1-4020-2265-4_9, 2005.

Foken, T., Aubinet, M., and Leuning, R.: The Eddy Covariance Method, in: Eddy Covariance: A Practical Guide to Measurement and Data Analysis, edited by Aubinet, M., Vesala, T., and Papale, D., Springer Atmospheric Sciences, pp. 1–19, Springer Netherlands, Dordrecht, https://doi.org/10.1007/978-94-007-2351-1_1, 2012a.

Foken, T., Leuning, R., Oncley, S. R., Mauder, M., and Aubinet, M.: Corrections and Data Quality Control, in: Eddy Covariance: A Practical Guide to Measurement and Data Analysis, edited by Aubinet, M., Vesala, T., and Papale, D., Springer Atmospheric Sciences, pp. 85–131, Springer Netherlands, Dordrecht, https://doi.org/10.1007/978-94-007-2351-1_4, 2012b.

Frenkiel, F. N. and Klebanoff, P. S.: Probability Distributions and Correlations in a Turbulent Boundary Layer, The Physics of Fluids, 16, 725–737, https://doi.org/10.1063/1.1694421, 1973.

Fuehrer, P. L. and Friehe, C. A.: Flux Corrections Revisited, Boundary-Layer Meteorology, 102, 415–458, https://doi.org/10.1023/A:1013826900579, 2002.

Greenhut, G. K. and Khalsa, S. J. S.: Updraft and Downdraft Events in the Atmospheric Boundary Layer Over the Equatorial Pacific Ocean, Journal of Atmospheric Sciences, 39, 1803–1818, https://doi.org/10.1175/1520-0469(1982)039<1803:UADEIT>2.0.CO;2, 1982.

Gu, L., Massman, W. J., Leuning, R., Pallardy, S. G., Meyers, T., Hanson, P. J., Riggs, J. S., Hosman, K. P., and Yang, B.: The Fundamental Equation of Eddy Covariance and Its Application in Flux Measurements, Agricultural and Forest Meteorology. 152: 135-148., pp. 135–148, https://doi.org/10.1016/j.agrformet.2011.09.014, 2012.

Heinesch, B., Yernaux, M., and Aubinet, M.: Some Methodological Questions Concerning Advection Measurements: A Case Study, Boundary-Layer Meteorology, 122, 457–478, https://doi.org/10.1007/s10546-006-9102-4, 2007.

Hicks, B. B. and Baldocchi, D. D.: Measurement of Fluxes Over Land: Capabilities, Origins, and Remaining Challenges, Boundary-Layer Meteorology, https://doi.org/10.1007/s10546-020-00531-y, 2020.

Hicks, B. B. and McMillen, R. T.: A Simulation of the Eddy Accumulation Method for Measuring Pollutant Fluxes, Journal of Climate and Applied Meteorology, 23, 637–643, https://doi.org/10.1175/1520-0450(1984)023<0637:ASOTEA>2.0.CO;2, 1984.

Hicks, B. B., Wesely, M. L., and Durham, J. L.: Critique of Methods to Measure Dry Deposition Workshop Summary, Tech. Rep. PB-81126443; EPA-600/9-80-050, Argonne National Lab., IL (USA); Environmental Protection Agency, Research Triangle Park, NC (USA), 1980.

Katsouvas, G. D., Helmis, C. G., and Wang, Q.: Quadrant Analysis of the Scalar and Momentum Fluxes in the Stable Marine Atmospheric Surface Layer, Boundary-Layer Meteorology, 124, 335–360, https://doi.org/10.1007/s10546-007-9169-6, 2007.

Katul, G., Kuhn, G., Schieldge, J., and Hsieh, C.-I.: The Ejection-Sweep Character of Scalar Fluxes in the Unstable Surface Layer, Boundary-Layer Meteorology, 83, 1–26, https://doi.org/10.1023/A:1000293516830, 1997.

Lee, X., Finnigan, J., and Paw U, K. T.: Coordinate Systems and Flux Bias Error, in: Handbook of Micrometeorology: A Guide for Surface Flux Measurement and Analysis, edited by Lee, X., Massman, W., and Law, B., Atmospheric and Oceanographic Sciences Library, pp. 33–66, Springer Netherlands, Dordrecht, https://doi.org/10.1007/1-4020-2265-4_3, 2005.

Lenschow, D. H., Mann, J., and Kristensen, L.: How Long Is Long Enough When Measuring Fluxes and Other Turbulence Statistics?, Journal of Atmospheric and Oceanic Technology, 11, 661–673, https://doi.org/10.1175/1520-0426(1994)011<0661:HLILEW>2.0.CO;2, 1994.

Leone, F. C., Nelson, L. S., and Nottingham, R. B.: The Folded Normal Distribution, Technometrics, 3, 543–550, https://doi.org/10.1080/00401706.1961.10489974, 1961.

McBean, G. A.: Comparison of the Turbulent Transfer Processes near the Surface, Boundary-Layer Meteorology, 4, 265–274, https://doi.org/10.1007/BF02265237, 1973.

Monin, A. S. and Obukhov, A. M.: Basic Laws of Turbulent Mixing in the Ground Layer of the Atmosphere, Translated for Geophysics Research Directorate, AF Cambridge Research Center ... by the American meteorological Society, Boston, MA, 1959.

Ohtaki, E.: On the Similarity in Atmospheric Fluctuations of Carbon Dioxide, Water Vapor and Temperature over Vegetated Fields, Boundary-Layer Meteorology, 32, 25–37, https://doi.org/10.1007/BF00120712, 1985.

Pattey, E., Desjardins, R. L., and Rochette, P.: Accuracy of the Relaxed Eddy-Accumulation Technique, Evaluated Using CO2 Flux Measurements, Boundary-Layer Meteorology, 66, 341–355, https://doi.org/10.1007/BF00712728, 1993.

Paw U, K. T., Baldocchi, D. D., Meyers, T. P., and Wilson, K. B.: Correction Of Eddy-Covariance Measurements Incorporating Both Advective Effects And Density Fluxes, Boundary-Layer Meteorology, 97, 487–511, https://doi.org/10.1023/A:1002786702909, 2000.

640 Rannik, Ü., Vesala, T., Peltola, O., Novick, K. A., Aurela, M., Järvi, L., Montagnani, L., Mölder, M., Peichl, M., Pilegaard, K., and Mammarella, I.: Impact of Coordinate Rotation on Eddy Covariance Fluxes at Complex Sites, Agricultural and Forest Meteorology, 287, 107 940, https://doi.org/10.1016/j.agrformet.2020.107940, 2020.

Raupach, M. R.: Conditional Statistics of Reynolds Stress in Rough-Wall and Smooth-Wall Turbulent Boundary Layers, Journal of Fluid Mechanics, 108, 363–382, https://doi.org/10.1017/S0022112081002164, 1981.

645 Rinne, H. J. I., Delany, A. C., Greenberg, J. P., and Guenther, A. B.: A True Eddy Accumulation System for Trace Gas Fluxes Using Disjunct Eddy Sampling Method, Journal of Geophysical Research: Atmospheres, 105, 24 791–24 798, https://doi.org/10.1029/2000JD900315, 2000a.

Rinne, J. and Ammann, C.: Disjunct Eddy Covariance Method, in: Eddy Covariance: A Practical Guide to Measurement and Data Analysis, edited by Aubinet, M., Vesala, T., and Papale, D., Springer Atmospheric Sciences, pp. 291–307, Springer Netherlands, Dordrecht,
650 https://doi.org/10.1007/978-94-007-2351-1_10, 2012.

Rinne, J., Tuovinen, J.-P., Laurila, T., Hakola, H., Aurela, M., and Hypén, H.: Measurements of Hydrocarbon Fluxes by a Gradient Method above a Northern Boreal Forest, Agricultural and Forest Meteorology, 102, 25–37, https://doi.org/10.1016/S0168-1923(00)00088-5, 2000b.

Siebicke, L. and Emad, A.: True Eddy Accumulation Trace Gas Flux Measurements: Proof of Concept, Atmospheric Measurement Techniques, 12, 4393–4420, https://doi.org/10.5194/amt-12-4393-2019, 2019.
655

Sun, J.: Tilt Corrections over Complex Terrain and Their Implication for CO2 Transport, Boundary-Layer Meteorology, 124, 143–159, https://doi.org/10.1007/s10546-007-9186-5, 2007.

Thomas, C. and Foken, T.: Flux Contribution of Coherent Structures and Its Implications for the Exchange of Energy and Matter in a Tall Spruce Canopy, Boundary-Layer Meteorology, 123, 317–337, https://doi.org/10.1007/s10546-006-9144-7, 2007.

660 Turnipseed, A. A., Pressley, S. N., Karl, T., Lamb, B., Nemitz, E., Allwine, E., Cooper, W. A., Shertz, S., and Guenther, A. B.: The Use of Disjunct Eddy Sampling Methods for the Determination of Ecosystem Level Fluxes of Trace Gases, Atmospheric Chemistry and Physics, 9, 981–994, https://doi.org/10.5194/acp-9-981-2009, 2009.

Webb, E. K., Pearman, G. I., and Leuning, R.: Correction of Flux Measurements for Density Effects Due to Heat and Water Vapour Transfer, Quarterly Journal of the Royal Meteorological Society, 106, 85–100, https://doi.org/10.1002/qj.49710644707, 1980.

665 Wesely, M. L.: Use of Variance Techniques to Measure Dry Air-Surface Exchange Rates, Boundary-Layer Meteorology, 44, 13–31, https://doi.org/10.1007/BF00117291, 1988.

Wilczak, J. M., Oncley, S. P., and Stage, S. A.: Sonic Anemometer Tilt Correction Algorithms, Boundary-Layer Meteorology, 99, 127–150, https://doi.org/10.1023/A:1018966204465, 2001.

Wyngaard, J. C. and Moeng, C.-H.: Parameterizing Turbulent Diffusion through the Joint Probability Density, Boundary-Layer Meteorology,
670 60, 1–13, https://doi.org/10.1007/BF00122059, 1992.

True eddy accumulation - Part 2: Theory and experiment of the short-time eddy accumulation method

Anas Emad[1] and Lukas Siebicke[1]

[1]Bioclimatology, University of Göttingen, Büsgenweg 2, 37077 Göttingen, Germany

Correspondence: Anas Emad (anas.emad@uni-goettingen.de)

Abstract. A new variant of the eddy accumulation method for measuring atmospheric exchange is derived and a prototype sampler is evaluated. The new method, termed short-time eddy accumulation (STEA), overcomes the requirement of fixed accumulation intervals in the true eddy accumulation method (TEA) and enables the sampling system to run in a continuous flow-through mode. STEA enables adaptive time-varying accumulation intervals which improves the system's dynamic range and brings many advantages to flux measurement and calculation.

The STEA method was successfully implemented and deployed to measure CO_2 fluxes over an agricultural field in Braunschweig, Germany. The measured fluxes matched very well against a conventional EC system (slope of 1.04, R^2 of 0.86). We provide a detailed description of the setup and operation of the STEA system in the continuous flow-through mode, devise an empirical correction for the effect of buffer volumes, and describe the important considerations for the successful operation of the STEA method.

The STEA method reduces the bias and uncertainty in the measured fluxes and creates new ways to design eddy accumulation systems with finer control over sampling and accumulation. The results encourage the application of STEA for measuring fluxes of more challenging atmospheric constituents such as reactive species.

1 Introduction

Micrometeorological methods provide non-invasive, in situ, integrated, and continuous point measurement for ecosystem fluxes on a scale ideal for ecosystem study (Baldocchi et al., 1988; Baldocchi, 2014). Among micrometeorological methods,

Monitoring the exchange of trace gases and energy between the earth's surface and the atmosphere is a key problem in ecology and climate science. The eddy covariance method (EC) has become the standard method for estimating the flux density on the scale of plant canopies (Baldocchi, 2014; Hicks and Baldocchi, 2020). The flux in the EC method is calculated as the covariance between the vertical wind velocity and the scalar concentration. For this, EC requires the availability of high-frequency measurements of the vertical wind velocity and the concentration of the atmospheric constituent (≥ 10 Hz). This requirement limits the EC method to few trace gases where fast-response gas analyzers are available. For constituents where only slow-response gas analyzers are available, several methods for measuring the fluxes exist (Rinne et al., 2021). Among these methods, the true eddy accumulation (TEA) (Desjardins, 1977) is the most direct and the closest to EC. TEA is formulated using similar principles and assumptions to the EC method. However, unlike EC, the TEA method requires the concentration measurements to be carried out once every averaging interval (30 minutes). For a long time, the development of the TEA method was hindered by the difficulty of fast air flow rate control and the strict operational requirements (Businger and Oncley, 1990; Hicks and McMillen, 1984). A recent improvement to the TEA method used a new type of mass flow controller, online coordinates rotation, and several online treatments of the signal to overcome important limitations of the method's applicability (Siebicke and Emad, 2019). The new system showed a good match with a reference eddy covariance system with coefficients of determination of up to 86% and a slope of 0.98. While this study demonstrated a successful proof-of-concept of TEA using modern sampling, it also showed that further research was required for continuous accumulation and long-term field operation, which we address with the current study.

The absence of high-frequency measurements of the scalar concentration creates unique challenges to the TEA method. The sampling decisions in TEA need to be done in real-time without complete knowledge of the wind statistics of the averaging interval. The problem of nonzero mean vertical wind velocity

60 ~~, and disjunct eddy accumulation (DEA) (Turnipseed et al., 2009).~~ , a direct consequence of this limitation, is discussed in the accompanying paper (Emad and Siebicke, 2022).

~~The reported bias on the flux due to nonzero $\bar{w}$ varied with different studies and accumulation methods. For TEA, Hicks and McMillen (19~~ ~~recommended that $\bar{w}$ should not exceed $0.0005\,\sigma_w$ if accumulated mass is measured and $0.02\,\sigma_w$ when concentrations are measured directly. Turnipseed et al. (2009) reported that a mean vertical wind bias of $\pm 0.25\,\sigma_w$ lead to $\pm 15\%$ errors in the~~

65 ~~flux using the disjunct eddy accumulation method. Values reported for the REA method showed that a loss of approximately 5% of the flux due to a $\bar{w}$ of $0.20\,\sigma_w$ (Pattey et al., 1993), which agrees with the recommendations of Businger and Oncley (1990). Additionally, the absence of high-frequency information means any decision on air sampling such as flow rate and sampling direction is final. The~~ Furthermore, the lack of high-frequency ~~information also~~ scalar measurements implies that sample accumulation ~~should~~ needs to happen on a time scale similar to the flux averaging interval (30 to 60 minutes). Therefore, imposing

70 a minimum limit on the sampling accumulation interval before the scalar concentration measurement can be conducted. ~~These limitations impose~~ This time limit imposes restrictive design considerations related to the size and function of sample accumulation reservoirs. ~~They also dictate~~ It dictates that the sampling apparatus needs to accommodate a large dynamic range ~~to~~ (up to $5\,\sigma_w$) to cover the range of wind velocities during the flux averaging interval ~~.~~ (Hicks and McMillen, 1984). The minimum time limit is also problematic if the sampled scalar changes in concentration over time, e.g., reactive species. Additionally, the

75 accumulation for long time intervals and the discontinuous nature of sample collection are particularly sensitive to instationary conditions in the accumulation apparatus (Siebicke and Emad, 2019). Additionally, the use of expandable bags in discrete sampling for the accumulation reservoirs has proven to be unreliable and prone to mechanical fatigue (Siebicke and Emad, 2019). Therefore, a more flexible approach is needed where the accumulation interval can be adapted to the requirements of the sampling system and the trace gas being measured.

80 ~~In this paper, we address these limitations of the TEA method.First, we revise the theory of true eddy accumulation and extend the TEA equation to non-ideal conditions . The new generalized TEA equation allows obtaining TEA fluxes equivalent to fluxes measured with EC when the vertical wind velocity is nonzero. This is achieved by incorporating knowledge about the scalar transport represented by the transport asymmetry coefficient. We show analytical and empirical ways to obtain the transport asymmetry coefficient and provide an interpretation of its value. Then, we describe the sensitivity of the flux to values~~

85 ~~of the transport asymmetry coefficient, the residual vertical mean velocity, and the different operational conditions~~ In this paper, we address these limitations by developing a novel method for eddy accumulation and providing a prototype implementation of such a system. ~~Next, we derived a new TEA method,~~ First, we derive a new eddy accumulation method, which we call the short-time eddy accumulation (STEA) ~~, which allows to carry out~~ . STEA method enables the sample accumulation ~~on variable intervals shorter than the flux averaging interval. We discuss the advantages and steps required to carry out flux measurements~~

90 ~~using the STEA method, different operational requirements,~~ to be carried out on variable shorter intervals which brings many improvements in the TEA flux measurements including the ability to accumulate samples in a continuous flow-through mode. Next, we discuss the effect of using buffer volumes on the concentration measurements and develop an empirical correction for the use of buffer volumes. Finally, we show a prototype and experimental measurements for CO_2 fluxes using the newly developed STEA method in the flow-through mode and compare the measured fluxes to reference EC measurements. We

95 discuss the advantages and steps required to carry out flux measurements using the STEA method, different constraints and operational requirements.

2 Theory

A detailed description of the TEA method derivation and assumptions is provided in the accompanying paper (Emad and Siebicke, 2022). Here we present a short overview to prepare for the short-time eddy accumulation derivation.

100 Under the assumptions of flow homogeneity and stationarity, the vertical exchange of the atmospheric scalar c is the flux across the measurement plane at height h, the flux F_c is (Finnigan et al., 2003; Gu et al., 2012)

$$F_c = \overline{cw} \tag{1}$$

Here, w is the vertical wind velocity $(\mathrm{m\,s^{-1}})$, c is the scalar density $(\mathrm{mol\,m^{-3}})$, and the over-bar denote time averages that follow Reynolds averaging rules.

105 The true eddy accumulation method is formulated by partitioning the average $\overline{wc}$ using the direction of the vertical wind velocity. Therefore, we write the flux as the expected value of the random variable wc conditional on the sign of the vertical wind velocity, $\mathrm{sign}(w)$

$$\overline{wc} = \overline{w^\uparrow c^\uparrow}\,\mathrm{P}(w^\uparrow) + \overline{w^\downarrow c^\downarrow}\,\mathrm{P}(w^\downarrow) \tag{2}$$

Where the arrows denote the direction of the vertical wind velocity, $\uparrow$ for updraft, and $\downarrow$ for downdraft. $\mathrm{P}(w^{\uparrow\downarrow})$ is the
110 probability that the observed wind velocity is in the respective direction. The TEA method makes use of this simple partitioning by physically realizing the terms $\overline{w^\uparrow c^\uparrow}$ and $\overline{w^\downarrow c^\downarrow}$ using sample accumulation instead of measuring individual realizations of w and c. For the practical implementation of the TEA system, a parameter A is necessary to relate the sampling flow rate to the measured w.

2.1 Short-time eddy accumulation

115 The original formulation of the true eddy accumulation method requires the samples to be accumulated for the entire averaging interval ~~T_{avg} before the measurement can take place. This can pose limitations on the operation and the applicability of the method.~~ Δt before the concentration measurement is ready for flux calculation. This limits the dynamic range and the flexibility of the sampling system.
~~We~~ To achieve a higher dynamic range for the sampling system and realize a more robust flow-through eddy accumulation
120 system, we propose a modification ~~for~~ to the TEA method ~~,~~ where samples can be accumulated for a sequence of shorter intervals τ_i that add up to the averaging period ~~T_{avg}.~~ Δt.

This formulation can be achieved by applying the law of total expectation to the random variable cw with respect to a partitioning variable Y that divides the averaging period ~~T_{avg}~~ Δt into multiple non-overlapping partitions with the length τ_i.

4

~~It follows that the expectation of cw is the conditional expected value of cw given Y and the flux is equal to~~ This partitioning scheme is applied individually to updarft and downdraft after partitioning with the direction of vertical wind velocity. Therefore, we write the expectation of $\overline{c^\uparrow w^\uparrow}$

$$\overline{cw} = \overline{\left(\overline{(cw)|Y}\right)} = \sum_i \overline{(cw)|Y_i}\, \mathrm{P}(Y_i)$$

$$\overline{c^\uparrow w^\uparrow} = \overline{\left(\overline{(c^\uparrow w^\uparrow)|Y}\right)} = \sum_i \overline{(c^\uparrow w^\uparrow)|Y_i}\, \mathrm{P}(Y_i) \tag{3}$$

~~This allows to write Eq. (??) as a sum of j intervals with the length of τ_i and a scaling factor A_i each. The concentration for either updraft or downdraft reservoirs can then be calculated from~~ The previous equation is similarly valid for the downdraft flux $\overline{c^\downarrow w^\downarrow}$. The measured concentration during a short averaging interval i, is given by

$$C^{\uparrow\downarrow} = \frac{1}{\sum_{i=1}^{i=j} A_i \overline{|w_i|}\tau_i} \sum_{i=1}^{i=j} \frac{1}{\int_t^{t+\tau_i} A_i|w|} \int_t^{t+\tau_i} A_i|w|\, c\, dt$$

$$C_i = \frac{\overline{cw|Y_i}}{\overline{|w|}} \tag{4}$$

The probability of the short averaging interval can be obtained easily, $\mathrm{P}(Y_i) = \tau_i/\Delta t$. V_i is the volume accumualted during the short interval i, defined as

$$V_i = A_i \int_t^{t+\tau_i} |w|\, \mathrm{d}t \tag{5}$$

The concentration in either updraft or downdraft reservoirs ~~at the end of the averaging interval is the~~ for the averaging interval Δt is the weighted mean of the short interval concentration measurements, C_i ~~weighted by the sample volume during the short interval V_i.~~

$$C^{\uparrow\downarrow} = \frac{1}{V_{total}} \sum_{i=1}^{i=j} C_i^{\uparrow\downarrow}\, V_i$$

$$C_{acc}^{\uparrow\downarrow} = \frac{1}{\overline{|w|}\Delta t} \sum_{i=1}^{i=j} C_i^{\uparrow\downarrow} \overline{|w_i|}\tau_i \tag{6}$$

145 ~~We call this new variety of eddy accumulation, the short-time eddy accumulation method (STEA)~~ We notice here that $\overline{|w_i|}\tau_i = V_i/A_i$ and $\overline{w}\Delta t = \sum_{i=1}^{i=j} V_i/A_i$.

The obtained $C_{acc}^{\uparrow}$ and $C_{acc}^{\downarrow}$ can be used to calculate the STEA flux (Emad and Siebicke, 2022)

$$F_{\text{STEA}} = \frac{C_{acc}^{\uparrow} V^{\uparrow} \left(\overline{|w|} - \bar{w}\right) - C_{acc}^{\downarrow} V^{\downarrow} \left(\overline{|w|} + \bar{w}\right)}{\overline{|w|} - \alpha_c \bar{w}} \times \frac{\overline{|w|}}{V_{total}} \tag{7}$$

Where F_{STEA} is the kinematic flux density $(\text{mol}\,\text{m}\,\text{s}^{-1})$. $C_{acc}^{\uparrow}$ and $C_{acc}^{\downarrow}$ are the mean molar densities $(\text{mol}\,\text{m}^{-3})$ of the
150 scalar c in updraft and downdraft reservoirs for the whole accumulation period Δt as calculated from Eq. 6. $V^{\uparrow}$ and $V^{\downarrow}$ are the accumulated sample volumes (m^3) in updraft and downdraft reservoirs during the averaging period. It is important here to use $V^{\uparrow}$ and $V^{\downarrow}$ as $\overline{|w|}\Delta t^{\uparrow}$ since the parameter A was not constant for different short intervals. $\overline{|w|}$ is the mean of the absolute vertical wind velocity $(\text{m}\,\text{s}^{-1})$ during the averaging period. $\bar{w}$ is the mean of the vertical wind velocity. α_c is the transport asymmetry coefficient for the scalar c (dimensionless).

2.2 Effect of buffer volumes

The short-time eddy accumulation method can be achieved in at least two ways, either using expandable buffer volumes (e.g., bags), which are emptied after each short interval measurement C_i or using a flow-through system with rigid buffer volumes. The flow-through system has ~~a practical operational benefit~~ practical operational benefits but requires additional correction to reverse the effect of buffer volumes on the concentration signal. Buffer volumes act as low pass filters (Cescatti et al., 2016).
160 They attenuate the magnitude of the high-frequency part and shift the phase of the signal. The buffer concentration at time step n is dependent on the new input sample concentration and the buffer concentration from the previous step $y[n-1]$. Thus, the buffer volume concentration y_n response to an input C_i can be described with the difference equation

$$y_{[n]} = C_{i[n]}\,\dot{q}_i + (1 - \dot{q}_i)\,y_{[n-1]} \tag{8}$$

where $\dot{q}$ is a dimensionless flow rate that is defined as the ratio between the sample mass to the total mass of air in the buffer
165 volume, at each time step n

$$\dot{q_n} = \frac{V_i\,\rho_i}{V_b\,\rho_b} \tag{9}$$

Where V_i and ρ_i are the volume and density of the ~~short accumulation sample , respectively, while~~ accumulated sample during the interval, i, respectively. V_b and ρ_b are the volume and the air density of the ~~buffer~~ air in the buffer volume, respectively. Equation (8) characterizes a first-order linear filter. The ~~treatment as a~~ short accumulated samples in the STEA method are
170 individually separated as they are forwarded to the gas analyzer, this discrete behavior is best modeled with a discrete-time ~~process aligns with the discrete operation of the STEA method .~~ system as shown in Eq. (8).

The system response is characterized by the dimensionless flow rate. The time constant of the system is defined as the required time for the system to reach $1/e$ from a step increase and relates to $\dot{q}$ by (Taylor et al., 2013).

$$\tau = -\frac{\Delta t}{\ln\left(1-\dot{q}\right)}.$$

$$\tau = -\frac{\Delta s}{\ln\left(1-\dot{q}\right)} \tag{10}$$

where Δt is the Δs is the length of the sampling interval.

Figure (1) shows the filter's magnitude and phase responses. The magnitude response $|H|$ plot shows how the magnitudes of different frequencies are attenuated, the smaller the dimensionless flow rate is, the larger the time constant is. Consequently, the attenuation is stronger.
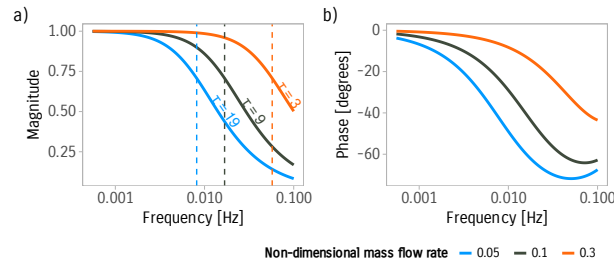
Figure 1. Frequency response for the first order linear filter used to model the buffer volumes for three different time constants. a) Magnitude response of the filter. Vertical dashed lines represent the cutoff frequencies for the respective time constants. b) Phase response of the filter.

2.3 Methods

2.3.1 Experimental site

Flux measurements were performed over a flat agricultural field of the Thünen Institute, located at 52.297 N, 10.449 E in Braunschweig, Germany. The site has an altitude of 76 m above sea level. During the measurement period, the fields south and north of the tower were planted with oats and corn, respectively. Both crops had a similar height of approximately 50 cm above the ground at the start of the comparison period.

2.3.2 Experiment period

The experiment started in September 2019. The first period (September 2019 to April 2020) was used for the development of the method which coincided with winter. The measurements during this period showed a lower quality and were excluded from the analysis.

7
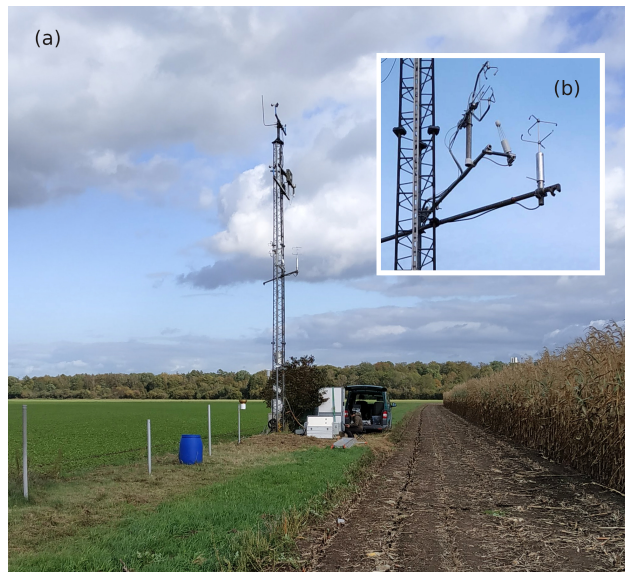
Figure 2. Photograph of the experimental field site showing the measurement tower **(a)** and a close up on the flux instruments mounted on the tower **(b)**.

~~The winter period was followed by a period of stable operation, running from May 2020 until October~~ Fluxes were measured throughout the year 2020. ~~During this period, we had a stable and continuous operation, however, intermittent discontinuities still existed due to blocked inlets, rain, or technical failures. From this period, we~~ We selected six weeks ~~in summer~~of good quality in summer based on instrument performance and weather conditions, spanning from 18 June 2020 to 31 July 2020 ~~,~~to compare the different methods.

2.3.3 Instruments

EC and STEA measurement complexes were mounted at 5 m height above the ground (Fig. 2). The instruments used in the experiment for flux measurements and data analysis are listed in Table 1. Meteorological variables were logged using a Sutron 9210 XLite logger (Sterling, USA). All the raw data needed for flux processing were synchronized on the STEA computer and remote servers for real-time processing.

The EC system comprised a dedicated sonic anemometer (uSonic-3 Omni H) and an open-path infra-red gas analyzer (IRGA). Wind and scalar density data were acquired at 20 Hz frequency. Relative to the Class-A sonic anemometer used for STEA, the northward, eastward, and vertical separation of the IRGA was -17 cm, 26 cm, and -15 cm, respectively. The Class-A sonic had a north offset azimuth of $90°$ degrees. Relative to the Omni-sonic anemometer used for EC, the northward, eastward, and vertical separation of the IRGA was 20 cm, -15.3 cm, and -20 cm. The north offset of the Omni-sonic was $169°$ degrees.

8

Table 1. Variables and instruments. Manufacturer key: METEK GmbH (Elmshorn, Germany), LI-COR Environmental Inc. (Lincoln, Nebraska, USA), LGR, (Los Gatos Research Inc., USA), Bosch (Bosch Sensortec GmbH, Germany), Vaisala (Helsinki, Finland), Kipp & Zonen (Delft - The Netherlands), Delta-T Devices Ltd (UK), Stevens Water Monitoring Systems, Inc (Oregon, USA), Texas Electronics (Dallas, USA)

Variable	Sensor	Manuf.	Method	Freq.
Wind u, v, w	uSonic-3 Omni H	METEK	EC	20 Hz
Sonic temp. Ts	uSonic-3 Omni H	METEK	EC	20 Hz
Wind u, v, w	uSonic-3 Class A	METEK	TEA	10 Hz
Sonic temp. Ts	uSonic-3 Class A	METEK	TEA	10 Hz
CO_2 density	LI-7500A	LI-COR	EC	10 Hz
H_2O density	LI-7500A	LI-COR	EC	10 Hz
CO_2 ppm	FGGA-24r-EP	LGR	TEA	1 Hz
H_2O ppm	FGGA-24r-EP	LGR	TEA	1 Hz
CH_4 ppm	FGGA-24r-EP	LGR	TEA	1 Hz
Air pressure P	BME280	Bosch	TEA	50 Hz
Air temperature	BME280	Bosch	TEA	50 Hz
Air humidity	HMP155	Vaisala	Meteo	10min
Air temperature	HMP155	Vaisala	Meteo	10min
Net radiation	CNR4	KIPP	Meteo	10min
Global radiation	BF5	DELTA-T	Meteo	10min
Soil heat flux	HFP01	LI-COR	Meteo	10min
Soil moisture	SDI-12	Stevens	Meteo	10min
Precipitation	TR-525M	Texas Elec.	Meteo	10min

2.4 ~~TEA~~ STEA system description

The ~~TEA~~ STEA system used in the experiment is based on an earlier system of Siebicke and Emad (2019). The new system used the same mass flow controllers and shared most of the operating software. It has, however, several differences and improvements. One major difference is the use of fixed stainless steel buffer volumes instead of expandable bags. The system was developed initially as a hybrid TEA-EC method to run the TEA method in a continuous flow-through mode (Siebicke, 2016). The system was set up to operate in the STEA continuous flow-through mode ~~described earlier in the theory section.~~. A constant duration for the short intervals (τ_i) equal to one minute was used. The STEA system is comprised of two identical sampling lines, one for updrafts and one for downdrafts. Each of the sampling lines has two rigid ~~buffers~~ buffer volumes in a sequence connected using 6 mm Teflon tube (Fig. 3).

The STEA sampling inlets were installed ~~in close proximity to~~ near the sonic's center of measurement volume. The horizontal separation was 22 cm, while the vertical separation between the two inlets was 2 cm. Upon sampling, the collected samples were carried using 6 mm Teflon tubes to the first set of buffers. The sampling can be summarized in the following steps (see a detailed description of the system operation and sampling in (Siebicke and Emad, 2019)):

1. 3D wind measurements are acquired from the sonic anemometer (uSonic-3 Class A) with a 10 Hz sampling frequency.
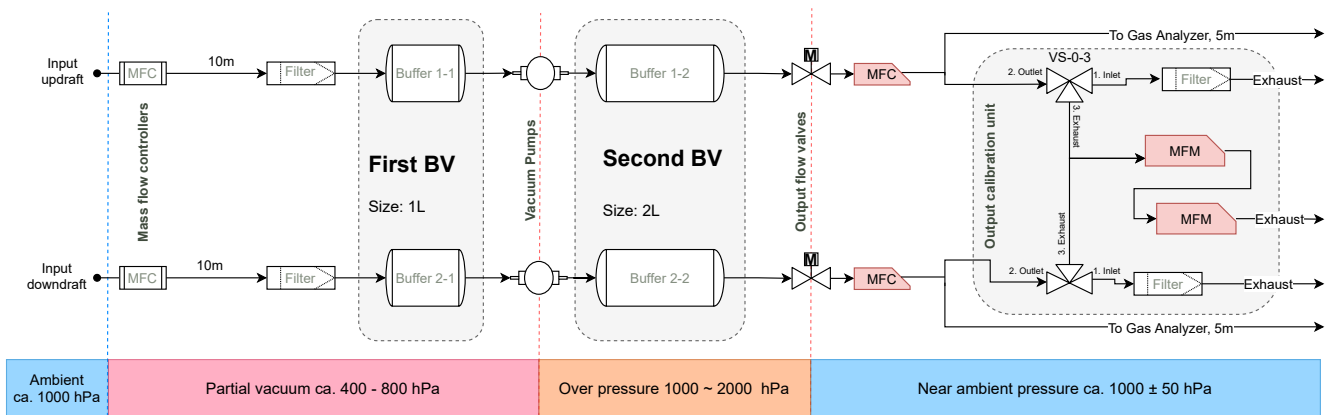
Figure 3. Functional and ~~hydraulic~~ pneumatic schematic of the implemented flow-through STEA system showing components, layout, properties, and operation conditions. Air samples are collected at the input and travel in distinct sampling lines for updrafts and downdrafts. Samples travel through tubes (lengths are shown), through filters, are then collected into two sets of buffer volumes shown here as *First BV* and *Second BV* separated by two vacuum pumps. The "Output flow valves" followed by mass flow controllers, control the output flow rate from the second set of buffers to the gas analyzers. Finally, samples can optionally be forwarded to a set of mass flow meters used for calibration purposes. The colored bottom bar below shows the range of pressure values at each stage.

2. Wind coordinates are rotated into the streamline coordinates using the planar fit method without an intercept (Dijk et al., 2004). The fit is performed online as a running window operation with a window width of 2 days and an update frequency of once every 30 minutes.

3. The mean vertical wind from the previous ~~window width (~~30 ~~min.)~~ minutes interval is removed to minimize $\overline{w}$. This is equivalent to applying a high-pass filter to the vertical wind velocity measurements.

4. ~~Sampling~~ The active sampling line is determined (updraft or downdraft) based on the direction of the rotated vertical wind velocity component.

5. ~~Sampling~~ The sampling scaling factor A_i is calculated based on wind conditions in the near past and the calibration coefficients of the mass flow controllers. The scaling factor should be constant during the short accumulation intervals.

6. Air samples are collected, the controllers are adjusted to collect an air sample with a volume equal to $A_i \, |w|$.

7. When enough sample volume is accumulated in the respective buffer volume, samples are forwarded to the gas analyzer for analysis. The amount of sample volume needed is determined based on the required flow rate for the gas analyzer and the time needed to flush the tubes and the measurement cell and to perform enough repeated measurements.

8. Mean concentrations of accumulated samples are measured. The slow gas analyzer (LGR FGGA-24r-EP) alternates on measuring the concentrations C_i of the accumulated samples for updraft and downdraft. The accumulation time

for the short intervals was set to a fixed interval of one minute instead of an adaptive interval duration. During each short interval, the gas analyzer performs repeated measurements for the gas concentration. The observed variability for repeated measurements in the short averaging intervals was SD = 0.501 ppm which was similar to the measured repeatability of the gas analyzer for a similar time interval.

2.5 STEA flux computations

This section describes the steps followed to obtain the final and corrected STEA flux. Firstly, we discuss the effect of water vapor on the measured concentrations of other scalars and how we corrected that remaining water cross-sensitivity. Then, we present the procedure of data quality screening. Next, we detail the steps of calculating the final STEA flux. Finally, we present the buffer volume empirical correction we applied.

2.5.1 Water vapor correction

The gas analyzer used for the STEA measurements (LGR FGGA-24r-EP) reports the molar fraction of CO_2 and CH_4 of moist air in parts per million (ppm). The measurements of CO_2 can not be used directly, as they are affected by the presence of water vapor. The presence of varying water vapor concentrations in the sample affects the measurements of CO_2 and CH_4 in cavity ring-down spectroscopy instruments in at least two ways: (i) the dilution effect, and (ii) the spectroscopic line broadening (Rella, 2010). Rella (2010) proposed a quadratic equation to correct for the combined effect of line broadening and water vapor dilution. The correction involves estimating ~~a~~ the parameters (a) and (b) in the equation

$$r_c = \frac{\chi_c}{1 + a\chi_w + b\chi_w^2} \tag{11}$$

where r_c is the dry mole fraction of the species c, χ_c is the wet mole fraction measured by the instrument, and χ_w is the water mole fraction measured by the instrument. For CO_2 measured by the LGR gas analyzer in ppm, Hiller et al. (2012) experimentally estimated theses coefficients as, ~~these coefficients were estimated as $a = -1.219 \times 10^{-06}(\pm 2.169 \times 10^{-09})$, $b = 1.229 \times 10^{-12}(\pm 1.073 \times 10^{-13})$ (Hiller et al., 2012) for where the unit is~~ $a = -1.219 \times 10^{-06}$, $b = 1.229 \times 10^{-12}$.

We found that using the same parameters could not control for all the effects of water. A linear slope different from zero was still found when supplying the gas analyzer with air of varying water ~~signal and~~ concentration and of constant CO_2. This suggests a remaining cross-sensitivity ~~on the presence~~ of CO_2 to the presence of water vapor. To control for this small remaining cross-sensitivity we used a linear fit to obtain the slope and ~~corrected for it~~ used it for the correction.

We were not able to supply the gas analyzer with air of known CO_2 ~~signal~~ concentration and varying water vapor. Instead, we used the ~~systems buffer volume to collect~~ system's buffer volumes to collect and pressurize air from the atmosphere, closed the inlets, and supplied the gas analyzer with enough sample flow rate for measurement. This procedure utilizes the effect of air drying due to decompression to deliver a varying water vapor content. Starting from humid atmospheric air near saturation ($RH \approx 90\%$, $T = 21\,°C$). Air is sucked and compressed into the stainless steel buffer volumes to a pressure of 2.6 bar. The water partial pressure in the pressurized buffers volumes will become higher than the saturation vapor pressure and water will

precipitate leading to dryer air. Air is then decompressed and forwarded to the analyzer. As the buffer pressure is reducing, water vapor content will increase to reach the same level of atmospheric humidity. Using this method we were able to modulate the water content in air from 6000 to 14000 ppm.

270 The accumulated sample was enough to supply the gas analyzer for ca. 10 min. We repeated the measurements several times and used the obtained dataset for correcting the ~~renaming~~ remaining cross-sensitivity using a linear fit.

2.5.2 Raw data quality screening

~~Raw data were processed to ensure the removal of~~ Raw measurements of the wind velocity and scalar concentration were screened for outliers due to measurement errors and ~~instruments~~ instrument malfunction. This included the following steps

275 – ~~Despiking:~~ Statistical screening: despiking, dropouts removal (Vickers and Mahrt, 1997), and plausibility limits of raw gas analyzer and wind measurements ~~are screened for outliers and removed following a procedure similar to Vickers and Mahrt (1997~~ (Sabbatini et al., 2018).

– ~~Dropouts removal: some sensors would get stuck on one value, the first value is kept and the rest are discarded.~~

– ~~Plausibility limits: values falling outside physical ranges were removed. Limits used are similar to those of Sabbatini et al. (2018)~~
280 ~~.~~

– ~~Deadband removal: measurement of~~ Flushing time removal: measurement of the short interval events involve regularly switching the sampling line coming to the gas analyzer ~~from updraft to~~ between updraft and downdraft reservoirs. This ~~will cause contamination from subsequent samples~~ caused subsequent samples to get contaminated. We experimentally chose a 25-second ~~deadband~~ threshold at the start of each short interval event to account for the flushing time. The
285 measurements falling ~~within the deadband were removed~~ before the threshold were discarded. Figure 4 shows an example of ~~deadband removal~~ discarded flushing times at the start of each averaging interval.

– Detection of sample contamination: periods where the flow rate to the gas analyzer is smaller than 400 mL min^{-1} are flagged. Under these conditions, ambient air might enter the system and contaminate the collected samples. When the number of flagged data points exceeds 10% of the total points in the sampling interval, data in the sampling interval are
290 discarded.

2.5.3 STEA flux calculation

After measurements are quality checked and erroneous data points are excluded, the final STEA flux is calculated as follows

– Short interval statistics: for each short interval sample, the gas analyzer will have several repeated measurements for the concentrations C_i, however, only one value is needed for the flux calculation. We use the median to obtain the
295 representative value in order to minimize uncertainty and exclude outliers. Figure 4 shows an example of data quality checking and choice.

12

- Calculate air molar volume: the molar volume of air is needed to express the flux in ~~dynamic flux units~~ units of $\mathrm{mol\,m^{-2}\,s^{-1}}$. The molar volume is calculated using sonic temperature, pressure, and humidity measurements.

- Calculate short intervals weights: following Eq. (~~??~~6), the measured short interval concentration should be weighted by the ratio of the accumulated volume during that interval to the total buffer volume V_i/V_{tot}.

- Calculate values of α_θ: values of α_θ are calculated using vertical wind velocity and sonic temperature measurements. Values of α_θ larger than 1 are discarded as they indicate a problem with the measurement.

- Calculate updraft and downdraft mean concentrations: $C^\uparrow_{acc}$ and $C^\uparrow_{acc}$ are calculated for the averaging period $\overset{\sim}{T_{avg}}\Delta t$.

- Calculate the flux: the STEA flux equation shown in Eq. (7) is used to obtain the final flux.
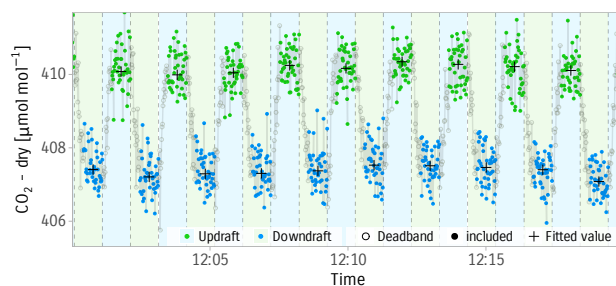
Figure 4. Data choice and fitting procedure for STEA method. Points represent consecutive concentration measurements from the gas analyzer. Updraft and downdraft samples are highlighted with blue and green, respectively. Grey hollow points are excluded from the data fitting (~~deadband~~flushing time). Cross points are the chosen representative concentrations for each short interval (the median). Further quality checks for raw data are outlined in Section 2.5.2. Data are from 21 June 2020 at mid day.

2.5.4 Buffer volume empirical correction

~~The use of buffer volumes introduces systematic biases to the fluxes.~~ Buffer volumes act on the signal as a low pass filter ~~. The time constant for the filter is needed to estimate the magnitude of filtering~~and introduce systematic bias to the fluxes. We used Eq. (10) to estimate the time constant of the ~~buffers~~buffer volumes used in our experiment. For each of the buffer volumes, a measurement point is acquired every two minutes. The mean dimensionless mass flow rate to the gas analyzer ~~is~~ was estimated from the pressure, the volume, and the estimated volumetric flow rate to the gas analyzer. ~~The average time constant was estimated to be 18 minutes.~~

We simulated the effect of buffer volumes on the high-frequency sonic temperature signal ~~. The loss in the fluxes was parameterized~~ and parameterized the flux loss by artificially degrading the sonic temperature in a procedure similar to Goulden et al. (1996) and Berger et al. (2001)

2.6 EC reference flux measurements and computations

The raw data from the two sonics and the high-frequency gas density measurements from the IRGA were used to compute eddy covariance fluxes for water vapor and CO_2 in the period from 1 April 2020 to 1 November 2020 using EddyPro® software (LI-COR Env. Inc. USA) version 7.0.4. The flux processing steps were chosen to be as similar as possible to the TEA processing scheme. The calculation of EC fluxes involved: statistical screening for the data quality issues following (Vickers and Mahrt, 1997), mean removal by block averaging, compensation of the time lag between the wind and the scalar time series using covariance maximization, tilt correction using the planar fit method without an intercept (Dijk et al., 2004) similar to TEA, and analytical high and low-frequency corrections to correct for the spectral attenuation of the IRGA (Moncrieff et al., 2005, 1997).

2.6.1 Density fluctuations correction

Due to using a closed-path gas analyzer, the TEA and STEA methods do not require WPL correction (Webb et al., 1980). WPL accounts for the effect of density fluctuations due to changes in temperature, humidity, and pressure. In TEA and STEA, after samples are collected and mixed in buffer volumes, the mean mixing ratio is measured. Therefore, no correction for density effects is needed. The measured TEA and STEA flux is equivalent to the flux measured with mixing ratios $\overline{r_c' w'}$.

2.7 Data selection for method comparison

For comparing the fluxes calculated from both methods, we selected averaging intervals according to the following criteria:

– Spike removal: following Vickers and Mahrt (1997) using a window width of 6 hours and a threshold of 2 standard deviations. This was mainly to account for unreliably elevated CO_2 concentration recorded by the open path gas analyzer due to water condensation.

– Rainy periods exclusion: data records during rainy weather conditions were excluded.

– Flux quality flags: periods where the flux quality flag is 1 or 2 according to Foken et al. (2005) were excluded.

– STEA low flow rate: averaging intervals flagged with the low flow rate flag described earlier were discarded.

After applying the above criteria, 992 averaging intervals remained. They accounted for 54.4% of the whole comparison period. Nighttime data were the majority of excluded values. only 33% of averaging intervals were valid during night-time compared to 70% during daytime. The open-path gas analyzer used for EC produced unreliable measurements during high humidity conditions at night due to water condensation. Table 2 shows a summary of data quality checks results.

Table 2. Summary of data quality checks for STEA and EC fluxes used in the EC/STEA flux intercomparison showing for each criterion, the number of averaging intervals that were excluded and the ratio of the excluded averaging intervals to the total. Details on the criteria and the thresholds used are provided in Sect. 3.3

Criteria	Averaging intervals	Ratio (%)
Spikes	3	0.2
EC missing value	~~25~~16	~~0.7~~0.9
~~Spikes 41 1.1~~Technical failure	~~75~~38	2.1
Rain	~~182~~91	5.0
STEA low flow rate	~~214~~107	5.9
Flux quality flag 2	~~390~~195	10.7
Flux quality flag 1	~~743~~382	~~20.4~~20.9
OK data	~~1971~~992	~~54.1~~54.4

To compare the overall difference between the two methods, we used the coefficient of determination R^2 and the slope of the orthogonal distance regression (ODR) (also known as major-axis regression and model II regression). ODR considers the errors in x and y as opposed to OLS regression which assumes the error in x is negligible (Wehr and Saleska, 2017).

3 Results and Discussion

We first discuss the ~~problem of nonzero mean vertical wind velocity and the new generalized TEA equation. Then, we discuss the value and interpretation of the transport asymmetry coefficient α. Next, we discuss the~~ newly proposed short-time eddy accumulation method. Then, we discuss some results and aspects of the STEA flux calculations. ~~Afterwards, we will~~ Afterward, we present the flux intercomparison between STEA and EC. Finally, we discuss the effect of using fixed buffer volumes on the fluxes and the proposed empirical correction.

3.1 Short-time Eddy Accumulation

~~We proposed the short-time eddy accumulation method (STEA), a modification of the TEA method where the accumulation time is divided into shorter intervals of time that add up to the flux averaging interval.~~

Using the STEA method reduced the dynamic range requirement for eddy accumulation sampling. For a short averaging interval of one minute, the range was on average 60% of the range required for the conventional eddy accumulation. As a result, the upper bound of the required dynamic range for w reported by Hicks and McMillen (1984) as $5\sigma_w$ is lowered to $3\sigma_w$. The reduction of the required dynamic range improves the accuracy and performance of the STEA system.

The accumulation on shorter time scales brings many advantages. First, it allows adapting to the local range of vertical wind velocity values which improves the resolution and dynamic range of the system. This can be achieved by exploiting the

autocorrelation of the wind velocity signal to predict a scaling parameter, A_i better adapted to the local velocity field for each interval. For a short interval, the range that the sampling apparatus ~~need~~ needs to cover will be on average smaller than the range of the whole averaging interval. ~~We found for a short averaging interval of one minute, the range was on average 60% smaller than that of the whole flux averaging interval. As a result, the upper bound of the required dynamic range for w reported by Hicks and McMillen (1984) as $5\sigma_w$ is lowered to $3.33\sigma_w$.~~

Additionally, the accumulation on varying intervals means the measurement frequency can be adjusted to match that of the gas analyzer or the precision requirements. This can be useful for reactive species and other ~~traces~~ trace gases, where relatively fast gas analyzers are available but not fast enough for EC.

Figure 5 demonstrates how the method works. In this example, the high-frequency samples are collected at 5 Hz frequency for a 30-minute long averaging interval. The averaging interval is divided into 30 short intervals with a duration varying from 70 to 190 seconds. The flux in this example equals $-14.24\,\mathrm{\mu mol\,m^{-2}\,s^{-1}}$.
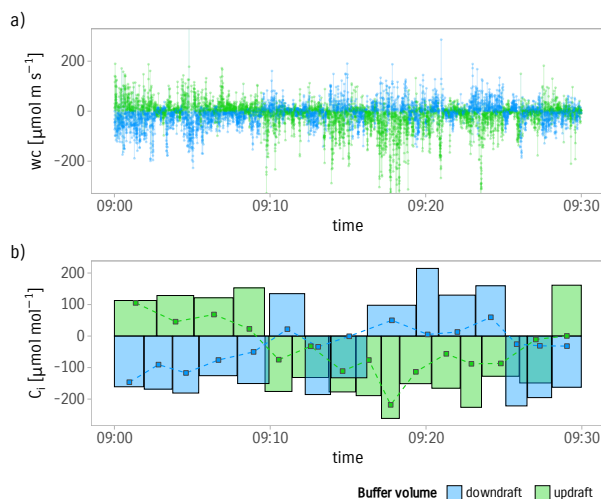
Figure 5. Sample accumulation using the STEA method. An example of 30 minutes of measurements: A) samples wc are collected based on wind direction and proportional to its magnitude; B) Short intervals are accumulated~~, the~~. The variable short interval duration guarantees equal accumulated volume for consecutive short intervals. Points are the concentrations C_i measured by the gas analyzer. The area of each rectangle represents the accumulated sample volume in arbitrary units and is equal to the relative weight for each concentration measurement. The sum of all measurements C_i weighted by the relative sample volume will equal the covariance. Data are from 20 June 2020.

Finally, the STEA method facilitates using the STEA system in a continuous flow-through mode using rigid reservoirs. The operation in flow-through mode requires two sets of buffer volumes in a series ~~.~~ as shown in Fig. 3. Two buffer volumes for each sampling line. The ideal operation of such a system can be achieved as follows:

1. Wind velocity is measured, rotated, and the value of the scaling parameter A_i is updated based on wind statistics and the flow calibration parameters.

2. ~~Air~~ For each sampling line, air samples are collected into the ~~first~~ respective set of buffer volumes ~~according to vertical wind sign~~ continuously according to the sign of the vertical wind velocity and proportional to ~~the vertical velocity~~ its magnitude and the value of A_i until a predefined accumulated volume is reached.

3. When the ~~goal~~ predefined accumulated volume is reached, the second ~~set of buffers~~ buffer volume in the sampling line is disconnected from the first. Sample accumulation time, τ_i and accumulated mass are recorded. ~~Samples~~ Then, samples are forwarded to the gas analyzer.

4. The slow gas analyzer alternates on measuring scalar concentration for each interval C_i from the second set of ~~buffers~~ buffer volumes for updraft and downdraft.

It is important for this scheme to keep the mass flow rate ~~to~~ of air from the second set of ~~buffers constant so that the assumption of time invariance of the linear filter used to model the buffers is not violated~~ buffer volumes to the gas analyzer constant for consecutive short intervals since the model used to represent the buffer volumes in Eq 8 assumes the flow rate to be constant with respect to time.

3.2 STEA fluxes computations

In this section, we ~~will~~ discuss some aspects related to the calculation of the STEA fluxes. We first discuss the effects of water vapor on CO_2 concentration measurements. Then, we discuss the effect of coordinates rotation on the fluxes. ~~Finally, we discuss the effect of density fluctuations on eddy accumulation methods.~~

3.2.1 Water vapor correction

Treatment of the residual cross-sensitivity of CO_2 on water ~~signal~~ vapor content using a linear fit produced a small slope of -1.17×10^{-4} shown in Fig. (6). Thus, a difference in water concentration of $4000\,\mathrm{ppm}$ between updraft and downdraft reservoirs, typically observed ~~at~~ in extreme conditions, will lead to a difference on the order of $0.5\,\mathrm{ppm}$ for CO_2.

Applying the water correction using the quadratic fit and the slope correction reduced the magnitude of STEA fluxes in comparison to the direct calculation of mixing ratios. However, it improved the fit between the STEA and the reference EC flux (Slope decreased from 1.18 to 1.04, and R^2 increased from ~~0.81 to 0.85~~ 0.80 to 0.86.)

3.2.2 Coordinates rotation

The online coordinates rotation produced ~~stable~~ stationary rotation angles over the experiment period. The eddy covariance fluxes calculated using the Class-A sonic using a two-month long dataset (1 June 2020 to 1 August 2020) produced the rotation angles: x-Pitch = $0.6°$; y-Roll = $-4.3°$ (using the YXZ Euler convention). Whereas for the TEA moving-window online rotation, larger pitch angles were observed with a mean of $3.6°$ and values slowly climbing from 1.2 to $6°$ during the 6 weeks comparison period. The roll angle ranged from $-0.9°$ to $-0.24°$ with an average of $-0.4°$.
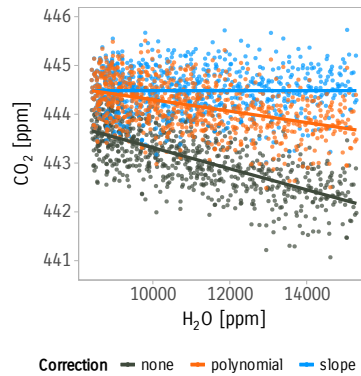
Figure 6. Effect of water correction on the measured CO_2 concentration using the LGR FGGA-24r-EP instrument. Points represent measured CO_2 by the gas analyzer when air with constant CO_2 concentration and varying H_2O concentration was supplied. Lines represent linear regression fits. Red colored points and line represent CO_2 measurements after applying the polynomial correction (Hiller et al., 2012; Rella, 2010). In blue are the CO_2 measurements after applying our slope adjustment correction to remove additional cross-sensitivity on water.

The use of online rotation with a moving window of two days minimized the residual ~~vertical mean~~ mean vertical wind in comparison to using the whole period of the experiment. This is likely due to a better adaptation to the local wind field. ~~The~~ Furthermore, the distribution of normalized mean vertical wind ~~values ranged from $-0.05\sigma_w$ to $0.38\sigma_w$ (mean magnitude of~~
410 ~~$0.251\sigma_w$) compared to $-0.04\sigma_w$ to $0.04\sigma_w$ (~~velocity of the short moving window had less spread, thinner tails and showed more symmetry around the mean compared to the whole-dataset rotation. The residual mean magnitude of ~~$0.06\sigma_w$) when using the online rotation with a~~ rotated w for the short moving window ~~.~~ was $0.04\sigma_w$, the first and third quartiles were -0.03 and 0.03. Whereas for the whole-dataset rotation, the mean magnitude was $0.17\sigma_w$ and the first and third quartiles were -0.07 and 0.22, respectively.

415 To estimate the effect of the online rotation method on the fluxes, we calculated EC fluxes using the two different rotation approaches while keeping other treatments constant. The comparison revealed that the online rotation with a moving window had minimal effect on the fluxes: a slope of approximately 1 and R^2 of 0.98 were obtained when using a linear fit. Nevertheless, this comparison only included data of good quality ~~. A comprehensive comparison might be needed to identify the effect under~~ from an ideal site. These results might differ for non-ideal conditions ~~.~~

420 **3.2.3** ~~Effect of density fluctuations~~

~~Changes in air density due to temperature, pressure, and dilution of water vapor and other gases bias the measured flux. If the density of a scalar is measured, a correction is needed to account for these effects (Webb et al., 1980). However, If the mixing ratio is measured, no correction is required since it is a conserved quantity. In TEA and STEA, after samples are collected and mixed in buffer volumes, the mean mixing ratio is measured. Therefore, no correction for density effects is needed. The~~
425 ~~resulting flux is equivalent to the flux measured with mixing ratios $\overline{r'_c w'}$. However, the density fluctuations might affect TEA~~

and STEA differently. Since, the mass flow rate of air is dependent on air density. The more dense the air is, the higher the mass flow rate is. If such an effect is not taken into account by using mass flow sampling, the resulting flux will be biased. The bias is equivalent to having the wind speed measurement dependent on air density in EC.

in a more complex site.

3.3 STEA/EC flux intercomparison

The measured CO_2 fluxes using the STEA method in flow-through mode showed a good match with the reference EC fluxes (Fig. (7)).
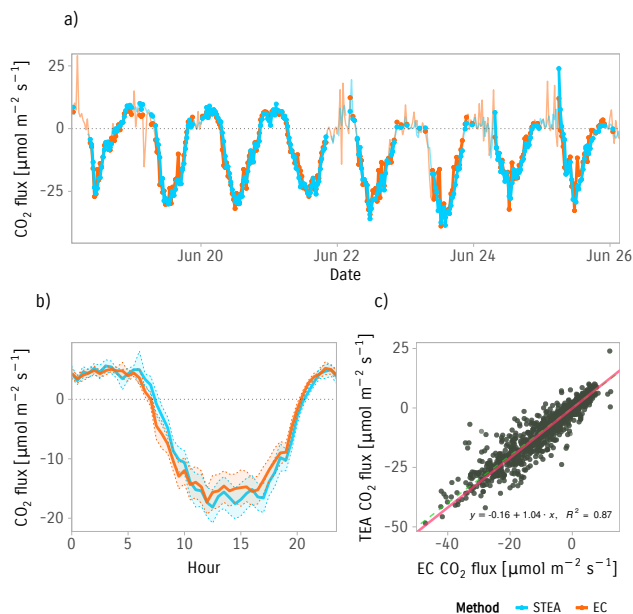
Figure 7. STEA and EC fluxes intercomparison. a) Time series of EC and STEA CO_2 fluxes for a subset period of 8 days. Points and thick lines indicate the averaging intervals used for comparison after filtering for quality. b) Mean diurnal cycle of CO_2 fluxes of STEA and EC. Bands are 95% confidence intervals of the mean calculated using nonparametric bootstrap. c) Scatter plot of STEA CO_2 fluxes against reference EC. The red line is the linear fit using the orthogonal distance regression (ODR). The dashed green line is a 1-to-1 line for reference.

The time series of measured CO_2 fluxes in Fig. (7 - a) shows that the STEA method was able to reproduce the daily dynamics of CO_2 flux very well. The estimated fluxes using the STEA method appear to have less fewer spikes and smoother in general, this is likely due to the smoothing effect of buffer volumes and the lower sensitivity of the closed path closed-path gas analyzer to rain and high humidity . in particular during nighttime. The correction for nonzero mean vertical wind velocity using α_θ was on average less than 1.5% of the flux magnitude. This is due to the ideal topography of the site and the online rotation of the coordinate. The correction at less ideal sites with more complex topography may differ.

19

The mean diurnal cycle estimates from the two methods ~~shown in Fig.~~ match very well (Fig. (7 - b)~~match very well~~). However,
a small time shift can be observed ~~on~~ in the mean diurnal cycle as a result of the phase shift introduced by the low-pass filtering effect of the buffer volumes.

The regression ~~results shown~~ in Fig. (7 - c) ~~show~~ shows that the measured CO_2 fluxes using the STEA method in flow-through mode have a very good agreement with the reference EC fluxes. The magnitude of STEA fluxes was comparable to EC fluxes (ODR slope = ~~1.05~~1.04). This indicates that the STEA method does not introduce systematic error to the fluxes. ~~However, the~~ The coefficient of determination R^2 was ~~0.87, which indicates a~~ 0.86 which is not uncommon for careful side-by-side multi-method or even single-method flux measurements. The remaining 13% ~~unexplained variance contributed by the uncertainty in the two estimates~~of unexplained variance is the joint contribution by the uncertainties of the two flux estimates from the EC and STEA methods. The observed uncertainty from the two methods calculated as the standard deviation of the difference was 4.36 $\mu\mathrm{mol\,m^{-2}\,s^{-1}}$.

We suggest three different mechanisms contributing to the observed uncertainty leading to the unexplained variance between the two estimates. First, the random sampling error arising from the stochasticity of turbulence (Hollinger and Richardson, 2005). The mean random sampling error of EC fluxes calculated following Finkelstein and Sims (2001) was 1.58 $\mu\mathrm{mol\,m^{-2}\,s^{-1}}$. The ~~observed uncertainty from the two methods calculated as the~~ standard deviation of the difference ~~is 4.29~~ between the two methods can be estimated to be 2.34 $\mu\mathrm{mol\,m^{-2}\,s^{-1}}$ ~~this is comparable to reported value of 2.7 using two tower estimates (Hollinger and Richardson, 2005). The errors also show~~ assuming the STEA fluxes have a similar random sampling error. Therefore, the random sampling error of the two methods accounts for more than half of the observed variance. The difference between the two methods also shows heteroscedasticity with the error increasing along with the absolute magnitude of the flux, a similar behavior of the random sampling error was observed by Hollinger and Richardson (2005) when comparing two tower estimates. The second source of uncertainty is the use of different gas analyzers for STEA and EC. Polonik et al. (2019) compared five different analyzers for measuring CO_2 fluxes. They showed that the root-mean-square error (RMSE) was in the range of 1 to 3.35 $\mu\mathrm{mol\,m^{-2}\,s^{-1}}$ depending on the analyzer type and the spectral correction method applied ~~.~~ with larger discrepancies observed when comparing open-path to closed-path sensors. Our results have an RMSE value of ~~4.3~~4.39 $\mu\mathrm{mol\,m^{-2}\,s^{-1}}$. While our result is slightly higher, it should be noted that RMSE is not an ideal metric for cross-studies comparison. A relative metric, such as R^2 would be more comparable but was unavailable. The third source of uncertainty is ~~due to~~ the use of buffer volumes in the STEA method. Figure (8 - a) demonstrates the increase of scatter in the measured fluxes due to the use of buffer volumes.

Finally, the different processing steps between the two methods can contribute to the uncertainty. In particular, the effects of time-lag compensation, spectral corrections, and statistical screening. We determined the combined effect of these processing treatments by calculating the EC flux with and without the treatments and found that the effect on the flux was negligible.

3.4 Effect of buffer volumes

Using fixed buffer volumes attenuates the signal. ~~The effect of buffer volumes can be described as a low-pass first-order linear filter. Figure (1) shows the filter's magnitude and phase responses. The magnitude response $|H|$ plot shows how the magnitudes~~

475 ~~Frequency response for the first order linear filter used to model the buffer volumes for three different time constants. a) Magnitude response of the filter. Vertical dashed lines represent the cutoff frequency for the respective time constant. b) Phase response of the filter.~~

To understand the effect of buffer volumes use on the measured scalar concentration~~. We~~, we carried out a simulation on a surrogate signal generated from sonic temperature. The simulation showed ~~the decline~~ that buffer volumes caused a decline

480 that can reach up to 10% of the fluxes under operation ranges similar to those of our experiment (for $\tau = 11$ minutes) (Fig. 8). The empirical correction was consistently able to mitigate most of the attenuation when the filter properties are assumed to be constant, (i.e, the flow rate needs to be constant for ~~each short interval~~consecutive short intervals). This assumption was difficult to maintain using the 1-minute switching regime. The simulation showed the empirical correction for the buffer volumes worked best when the correction factor was obtained using a linear fit, as opposed to taking a ratio of the attenuated

485 flux to the true flux for each averaging interval. The correction factor, in this case, is the reciprocal of the slope of the linear regression between the attenuated flux and the true flux. The correction factor calculated using Eq. (8) shows a good agreement between sensible heat flux and CO_2. However, the uncertainty of the correction factor increased with increasing buffer volume time constant. For our experiment, the average time constant for the first-order linear filter used to model the buffer volume was estimated to be $\tau = 700$ seconds. This value was used to simulate the loss on the fluxes using the sensible heat flux calculated

490 from the sonic anemometer. The correction factor was obtained from the slope of the attenuated flux and was equal to 1.18
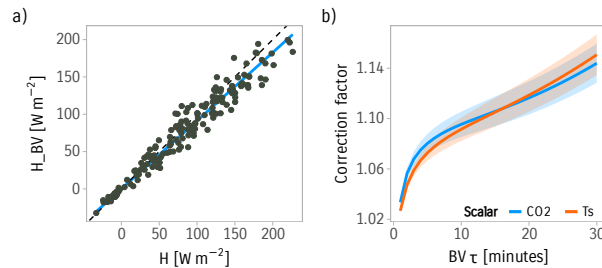
Figure 8. Empirical buffer volume correction. a) Effect of buffer volume attenuation on sensible heat flux with a time constant $\tau = 11$ minutes. The blue solid line is the linear fit between the two. b) Empirical correction factor for the effect of buffer volumes calculated as the reciprocal of the slope of attenuated flux for CO_2 and sensible heat flux. Bands are the estimated slope $\pm$ one standard error of the slope.

4 Conclusions

In this paper, we ~~revised the theory of the true eddy accumulation method and extended the applicability of the method to non-ideal conditions where the mean vertical wind velocity during the averaging interval is not zero. The new generalized~~

~~equation allows estimating the scalar mean during the flux averaging interval and define conditions where the error in the~~
495 ~~flux is significant. We found that the error in the TEA flux is a function of the disparity of atmospheric transport and defined ways and conditions to constrain that error. We found that it is possible to achieve minimum bias in the TEA flux under most atmospheric conditions. We believe these results increase the confidence in using the TEA method for different atmospheric constituents and under a variety of atmospheric conditions.~~

~~Additionally, we~~ proposed an alternative method for the measurement of ecosystem-level fluxes. The new method, referred to
500 here as short-time eddy accumulation (STEA), allows the sample accumulation to be carried out on shorter varying-length intervals. The STEA method offers more flexibility than ~~TEA~~ the traditional TEA method and has many potential benefits~~including a better~~. Most importantly, STEA provides a higher dynamic range and ~~higher~~ better accuracy than the TEA method~~, and the ability to operate~~. It enables operating sample accumulation under a flow-through scheme using fixed buffer volumes. The flexibility introduced by the ~~new~~ STEA method offers new ways to design eddy accumulation systems that are particularly suited
505 for ~~a specific atmospheric constituent or a specific gas analyzer~~specific atmospheric constituents gas analyzers. For example, the accumulation time can be tailored to measure reactive species with lifetimes shorter than a conventional flux integration interval or to distribute the gas analyzer time to measure ~~the~~ fluxes at different heights.

Furthermore, we presented a prototype evaluation of the STEA method under the flow-through regime. We described the details of the system design and operation. We compared flux measurements from our new system against a reference EC
510 system over a flat agricultural field. The fluxes from the two methods were in very good agreement. We highlighted the importance of different processing and design aspects between the two methods and their potential ~~effect~~ effects on the fluxes.

Finally, we analyzed the effect of buffer volumes in the flow-through operational mode on the fluxes and proposed an empirical correction to correct for the underestimation resulting from the low-pass filtering behavior of the buffer volumes.

In summary, the ~~generalized TEA equation and the~~ new STEA method ~~provide~~ provides a direct flux measurement ~~methods~~
515 ~~that complement~~ method that complements the state-of-the-art EC method. ~~They extend~~ It extends the coverage of micrometeorological methods to new trace gases and atmospheric constituents beyond the scope of the EC method.

520 **Appendix A: List of symbols**

Table A1. Symbols and subscripts with units

Symbols

c	$\mathrm{mol\,m^{-3}}$	Molar density of a scalar
w	$\mathrm{m\,s^{-1}}$	Vertical wind velocity
~~T_{avg}~~ Δt	s	Flux averaging interval
A	–	TEA sampling scaling factor
V	$\mathrm{m^3}$	Volume
C	$\mathrm{mol\,m^{-3}}$	Mean concentration of accumulated samples
α_c	–	Transport asymmetry coefficient for scalar c
ρ	–	~~Corelation~~ Correlation coefficient
$\dot{q}$	–	Dimensionless mass flow rate
τ	s	Time constant of the buffer volume
r_c	ppm	Mixing ratio in dry air for a scalar, c

Subscripts

acc	Accumulated samples
$\uparrow$	Updraft buffer volume
$\downarrow$	Downdraft buffer volume
c	Atmospheric constituent

the idea of flow-through eddy accumulation system, build the TEA system used in the experiment, planned and supervised the experiment, provided feedback on the results, the analysis, and the manuscript.

535

References

Baldocchi, D.: Measuring Fluxes of Trace Gases and Energy between Ecosystems and the Atmosphere - the State and Future of the Eddy Covariance Method, Global Change Biology, 20, 3600–3609, https://doi.org/10.1111/gcb.12649, 2014.

Baldocchi, D. D., Hicks, B. B., and Meyers, T. P.: Measuring Biosphere-Atmosphere Exchanges of Biologically Related Gases with Microm-
540   eteorological Methods, Ecology, 69, 1331–1340, https://doi.org/10.2307/1941631, 1988.

Berger, B. W., Davis, K. J., Yi, C., Bakwin, P. S., and Zhao, C. L.: Long-Term Carbon Dioxide Fluxes from a Very Tall Tower in a Northern Forest: Flux Measurement Methodology, Journal of Atmospheric and Oceanic Technology, 18, 529–542, https://doi.org/10.1175/1520-0426(2001)018<0529:LTCDFF>2.0.CO;2, 2001.

Bowling, D. R., Turnipseed, A. A., Delany, A. C., Baldocchi, D. D., Greenberg, J. P., and Monson, R. K.: The Use of Relaxed Eddy
545   Accumulation to Measure Biosphere-Atmosphere Exchange of Isoprene and Other Biological Trace Gases, Oecologia, 116, 306–315, https://doi.org/10.1007/s004420050592, 1998.

Businger, J. A. and Oncley, S. P.: Flux Measurement with Conditional Sampling, Journal of Atmospheric and Oceanic Technology, 7, 349–352, https://doi.org/10.1175/1520-0426(1990)007<0349:FMWCS>2.0.CO;2, 1990.

Cescatti, A., Marcolla, B., Goded, I., and Gruening, C.: Optimal Use of Buffer Volumes for the Measurement of Atmospheric Gas Con-
550   centration in Multi-Point Systems, Atmospheric Measurement Techniques Discussions, pp. 1–16, https://doi.org/10.5194/amt-2016-18, 2016.

Desjardins, R. L.: Energy Budget by an Eddy Correlation Method, Journal of Applied Meteorology, 16, 248–250, https://doi.org/10.1175/1520-0450(1977)016<0248:EBBAEC>2.0.CO;2, 1977.

Dijk, A., Moene, A., and de Bruin, H.: The Principles of Surface Flux Physics: Theory, Practice and Description of the ECPACK Library,
555   The Principles of Surface Flux Physics: Theory, Practice and Description of the ECPACK Library, 2004.

Emad, A. and Siebicke, L.: Replication Code for: Advances in the True Eddy Accumulation Method: New Theory, Implementation, and Field Results, https://doi.org/10.25625/SYQITK, 2021a.

Emad, A. and Siebicke, L.: Replication Data for: Advances in the True Eddy Accumulation Method: New Theory, Implementation, and Field Results, https://doi.org/10.25625/IVTS87, 2021b.

560   Emad, A. and Siebicke, L.: True Eddy Accumulation - Part 1: Solutions to the Problem of Non-Vanishing Mean Vertical Wind Velocity [Submitted along This Paper], Atmospheric Measurement Techniques Discussions, 2022.

Finkelstein, P. L. and Sims, P. F.: Sampling Error in Eddy Correlation Flux Measurements, Journal of Geophysical Research: Atmospheres, 106, 3503–3509, https://doi.org/10.1029/2000JD900731, 2001.

Finnigan, J. J., Clement, R., Malhi, Y., Leuning, R., and Cleugh, H.: A Re-Evaluation of Long-Term Flux Measurement Techniques Part I:
565   Averaging and Coordinate Rotation, Boundary-Layer Meteorology, 107, 1–48, https://doi.org/10.1023/A:1021554900225, 2003.

Foken, T., Göckede, M., Mauder, M., Mahrt, L., Amiro, B., and Munger, W.: Post-Field Data Quality Control, in: Handbook of Microm-
eteorology: A Guide for Surface Flux Measurement and Analysis, edited by Lee, X., Massman, W., and Law, B., Atmospheric and Oceanographic Sciences Library, pp. 181–208, Springer Netherlands, Dordrecht, https://doi.org/10.1007/1-4020-2265-4_9, 2005.

Goulden, M. L., Munger, J. W., Fan, S.-M., Daube, B. C., and Wofsy, S. C.: Measurements of Carbon Sequestration by Long-Term
570   Eddy Covariance: Methods and a Critical Evaluation of Accuracy, Global Change Biology, 2, 169–182, https://doi.org/10.1111/j.1365-2486.1996.tb00070.x, 1996.

Gu, L., Massman, W. J., Leuning, R., Pallardy, S. G., Meyers, T., Hanson, P. J., Riggs, J. S., Hosman, K. P., and Yang, B.: The Fundamental Equation of Eddy Covariance and Its Application in Flux Measurements, Agricultural and Forest Meteorology. 152: 135-148., pp. 135–148, https://doi.org/10.1016/j.agrformet.2011.09.014, 2012.

575   Hicks, B. B. and Baldocchi, D. D.: Measurement of Fluxes Over Land: Capabilities, Origins, and Remaining Challenges, Boundary-Layer Meteorology, https://doi.org/10.1007/s10546-020-00531-y, 2020.

Hicks, B. B. and McMillen, R. T.: A Simulation of the Eddy Accumulation Method for Measuring Pollutant Fluxes, Journal of Climate and Applied Meteorology, 23, 637–643, https://doi.org/10.1175/1520-0450(1984)023<0637:ASOTEA>2.0.CO;2, 1984.

Hiller, R. V., Zellweger, C., Knohl, A., and Eugster, W.: Flux Correction for Closed-Path Laser Spectrometers without Internal Water Vapor
580   Measurements, Atmospheric Measurement Techniques Discussions, 5, 351–384, https://doi.org/10.5194/amtd-5-351-2012, 2012.

Hollinger, D. Y. and Richardson, A. D.: Uncertainty in Eddy Covariance Measurements and Its Application to Physiological Models, Tree Physiology, 25, 873–885, https://doi.org/10.1093/treephys/25.7.873, 2005.

Lenschow, D. H., Mann, J., and Kristensen, L.: How Long Is Long Enough When Measuring Fluxes and Other Turbulence Statistics?, Journal of Atmospheric and Oceanic Technology, 11, 661–673, https://doi.org/10.1175/1520-0426(1994)011<0661:HLILEW>2.0.CO;2, 1994.

585   Moncrieff, J., Clement, R., Finnigan, J., and Meyers, T.: Averaging, Detrending, and Filtering of Eddy Covariance Time Series, in: Handbook of Micrometeorology: A Guide for Surface Flux Measurement and Analysis, edited by Lee, X., Massman, W., and Law, B., Atmospheric and Oceanographic Sciences Library, pp. 7–31, Springer Netherlands, Dordrecht, https://doi.org/10.1007/1-4020-2265-4_2, 2005.

Moncrieff, J. B., Massheder, J. M., de Bruin, H., Elbers, J., Friborg, T., Heusinkveld, B., Kabat, P., Scott, S., Soegaard, H., and Verhoef, A.: A System to Measure Surface Fluxes of Momentum, Sensible Heat, Water Vapour and Carbon Dioxide, Journal of Hydrology, 188–189,
590   589–611, https://doi.org/10.1016/S0022-1694(96)03194-0, 1997.

Monin, A. S. and Obukhov, A. M.: Basic Laws of Turbulent Mixing in the Ground Layer of the Atmosphere, Translated for Geophysics Research Directorate, AF Cambridge Research Center ... by the American meteorological Society, Boston, MA, 1959.

Pattey, E., Desjardins, R. L., and Rochette, P.: Accuracy of the Relaxed Eddy-Accumulation Technique, Evaluated Using CO2 Flux Measurements, Boundary-Layer Meteorology, 66, 341–355, https://doi.org/10.1007/BF00712728, 1993.

595   Polonik, P., Chan, W. S., Billesbach, D. P., Burba, G., Li, J., Nottrott, A., Bogoev, I., Conrad, B., and Biraud, S. C.: Comparison of Gas Analyzers for Eddy Covariance: Effects of Analyzer Type and Spectral Corrections on Fluxes, Agricultural and Forest Meteorology, 272–273, 128–142, https://doi.org/10.1016/j.agrformet.2019.02.010, 2019.

Rella, C.: Accurate Greenhouse Gas Measurements in Humid Gas Streams Using the Picarro G1301 Carbon Dioxide / Methane / Water Vapor Gas Analyzer, White paper, Picarro Inc, Sunnyvale, CA, USA, p. 18, 2010.

600   Rinne, H. J. I., Delany, A. C., Greenberg, J. P., and Guenther, A. B.: A True Eddy Accumulation System for Trace Gas Fluxes Using Disjunct Eddy Sampling Method, Journal of Geophysical Research: Atmospheres, 105, 24 791–24 798, https://doi.org/10.1029/2000JD900315, 2000a.

Rinne, J. and Ammann, C.: Disjunct Eddy Covariance Method, in: Eddy Covariance: A Practical Guide to Measurement and Data Analysis, edited by Aubinet, M., Vesala, T., and Papale, D., Springer Atmospheric Sciences, pp. 291–307, Springer Netherlands, Dordrecht,
605   https://doi.org/10.1007/978-94-007-2351-1_10, 2012.

Rinne, J., Tuovinen, J.-P., Laurila, T., Hakola, H., Aurela, M., and Hypén, H.: Measurements of Hydrocarbon Fluxes by a Gradient Method above a Northern Boreal Forest, Agricultural and Forest Meteorology, 102, 25–37, https://doi.org/10.1016/S0168-1923(00)00088-5, 2000b.

Rinne, J., Ammann, C., Pattey, E., Paw U, K. T., and Desjardins, R. L.: Alternative Turbulent Trace Gas Flux Measurement Methods, in: Springer Handbook of Atmospheric Measurements, edited by Foken, T., Springer Handbooks, pp. 1505–1530, Springer International Publishing, Cham, https://doi.org/10.1007/978-3-030-52171-4_56, 2021.

Sabbatini, S., Mammarella, I., Arriga, N., Fratini, G., Graf, A., Hörtnagl, L., Ibrom, A., Longdoz, B., Mauder, M., Merbold, L., Metzger, S., Montagnani, L., Pitacco, A., Rebmann, C., Sedlák, P., Šigut, L., Vitale, D., and Papale, D.: Eddy Covariance Raw Data Processing for CO2 and Energy Fluxes Calculation at ICOS Ecosystem Stations, International Agrophysics, 32, 495–515, https://doi.org/10.1515/intag-2017-0043, 2018.

Siebicke, L.: A True Eddy Accumulation -Eddy Covariance Hybrid for Measurements of Turbulent Trace Gas Fluxes, Geophysical Research Abstracts EGU General Assembly, 18, 2016–16 124, 2016.

Siebicke, L. and Emad, A.: True Eddy Accumulation Trace Gas Flux Measurements: Proof of Concept, Atmospheric Measurement Techniques, 12, 4393–4420, https://doi.org/10.5194/amt-12-4393-2019, 2019.

Taylor, C. J., Young, P. C., and Chotai, A.: True Digital Control: Statistical Modelling and Non-Minimal State Space Design, Wiley, 1st edition edn., 2013.

Turnipseed, A. A., Pressley, S. N., Karl, T., Lamb, B., Nemitz, E., Allwine, E., Cooper, W. A., Shertz, S., and Guenther, A. B.: The Use of Disjunct Eddy Sampling Methods for the Determination of Ecosystem Level Fluxes of Trace Gases, Atmospheric Chemistry and Physics, 9, 981–994, https://doi.org/10.5194/acp-9-981-2009, 2009.

Vickers, D. and Mahrt, L.: Quality Control and Flux Sampling Problems for Tower and Aircraft Data, Journal of Atmospheric and Oceanic Technology, 14, 512–526, https://doi.org/10.1175/1520-0426(1997)014<0512:QCAFSP>2.0.CO;2, 1997.

Webb, E. K., Pearman, G. I., and Leuning, R.: Correction of Flux Measurements for Density Effects Due to Heat and Water Vapour Transfer, Quarterly Journal of the Royal Meteorological Society, 106, 85–100, https://doi.org/10.1002/qj.49710644707, 1980.

Wehr, R. and Saleska, S. R.: The Long-Solved Problem of the Best-Fit Straight Line: Application to Isotopic Mixing Lines, Biogeosciences, 14, 17–29, https://doi.org/10.5194/bg-14-17-2017, 2017.